2009-01-1921

Hydrogen SI and HCCI Combustion in a Direct-Injection Optical Engine

M.F. Rosati and P.G. Aleiferis
University College London, UK

ABSTRACT

Hydrogen has been largely proposed as a possible alternative fuel for internal combustion engines. Its wide flammability range allows higher engine efficiency with leaner operation than conventional fuels, for both reduced toxic emissions and no CO_2 gases. Independently, Homogenous Charge Compression Ignition (HCCI) also allows higher thermal efficiency and lower fuel consumption with reduced NO_X emissions when compared to Spark-Ignition (SI) engine operation. For HCCI combustion, a mixture of air and fuel is supplied to the cylinder and autoignition occurs from compression; engine is operated throttle-less and load is controlled by the quality of the mixture, avoiding the large fluid-dynamic losses in the intake manifold of SI engines. HCCI can be induced and controlled by varying the mixture temperature, either by Exhaust Gas Recirculation (EGR) or intake air pre-heating. A combination of HCCI combustion with hydrogen fuelling has great potential for virtually zero CO_2 and NO_X emissions. Nevertheless, combustion on such a fast burning fuel with wide flammability limits and high octane number implies many disadvantages, such as control of backfiring and speed of autoignition and there is almost no literature on the subject, particularly in optical engines. Experiments were conducted in a single-cylinder research engine equipped with both Port Fuel Injection (PFI) and Direct Injection (DI) systems running at 1000 RPM. Optical access to in-cylinder phenomena was enabled through an extended piston and optical crown. Combustion images were acquired by a high-speed camera at 1° or 2° crank angle resolution for a series of engine cycles. Spark-ignition tests were initially carried out to benchmark the operation of the engine with hydrogen against gasoline. DI of hydrogen after intake valve closure was found to be preferable in order to overcome problems related to backfiring and air displacement from hydrogen's low density. HCCI combustion of hydrogen was initially enabled by means of a pilot port injection of n-heptane preceding the main direct injection of hydrogen, along with intake air pre-heating. Sole hydrogen fuelling HCCI was finally achieved and made sustainable, even at the low compression ratio of the optical engine by means of closed-valve DI, in synergy with air-pre-heating and negative valve overlap to promote internal EGR. Various operating conditions were analysed, such as fuelling in the range of air excess ratio 1.2–3.0 and intake air temperatures of 200–400 °C. Finally, both single and double injections per cycle were compared to identify their effects on combustion development.

INTRODUCTION

BACKGROUND

Hydrogen has been suggested as a possible replacement for most fuels used today and can be produced from fossil fuels and sustainable methods in many different ways: from natural gas, biomass, or wind and solar energy through electrolysis of water. The main advantage of burning hydrogen in internal combustion engines is its lack of carbon content, leading to total absence of Particulate Matter (PM), Unburned Hydro-Carbons (UHC), CO and CO_2 exhaust emissions. In fact, the idea of an internal combustion engine running on pure hydrogen is as old as the engine itself. Cecil was probably the first to recommend the use of hydrogen as a fuel for powering engines [1]. Nicolaus Otto himself (1832–1891) worked with synthetic producer gas, which probably contained more than 50% hydrogen [2].

The Engineering Meetings Board has approved this paper for publication. It has successfully completed SAE's peer review process under the supervision of the session organizer. This process requires a minimum of three (3) reviews by industry experts.

ISSN 0148-7191

SAE Customer Service: Tel: 877-606-7323 (inside USA and Canada)
Tel: 724-776-4970 (outside USA)
Fax: 724-776-0790
Email: CustomerService@sae.org
SAE Web Address: http://www.sae.org

Printed in USA

The lack of established technology necessary to handle specific difficulties associated with the properties of hydrogen, as well as the diversity of strong political opinions and projected infrastructure costs for the safe production and delivery of hydrogen on a large scale, have discouraged most automotive manufacturers for many years from promoting hydrogen as a fuel for their internal combustion engines. However, automotive manufacturers are seriously challenged today not only by legislative demands of low emissions but also by the need to decrease their dependency on non-renewable fuels, therefore, hydrogen has recently been the subject of much discussion, research and publications. In the past few years, research on hydrogen engines has been reported by several engine manufacturers [3–8], with BMW leading the way [9–12].

Hydrogen has several unique properties, most of which are quite different from conventional fuels. Some of these properties are summarized in Table 1 [12–16]. Hydrogen has very low density and, although its heating value on a mass basis is very high in comparison to other fuels (120 MJ/kg for hydrogen, 43.5 MJ/kg for gasoline), on a volume basis this is the lowest among common fuels (10.2 MJ/m^3 for hydrogen, 216.4 MJ/m^3 for gasoline). However, hydrogen has a wide range of flammability and its minimum ignition energy is about one order of magnitude less than that required for gasoline. Additionally, the autoignition temperature of hydrogen is relatively high. This allows larger compression ratios to be used in hydrogen engines for higher efficiency. Hydrogen's flame speed is nearly one order of magnitude higher than that of gasoline and other hydrocarbon fuels. For leaner mixtures, however, flame velocity decreases significantly. Its adiabatic flame temperature is generally higher than that of other fuels. Hydrogen also has some very high values of key transport properties, such as kinematic viscosity, thermal conductivity and diffusion coefficient. These differences lead to a Lewis number that is lower than that of most common fuels and contribute substantially to the unique combustion characteristics of hydrogen [17–18].

These facts mostly dictate that hydrogen is an excellent fuel for satisfactory performance in engine applications. However, there are various challenging issues associated with putting hydrogen to practice in internal combustion engines, *e.g.* high pressure rise, occurrence of pre-ignition/knocking in the combustion chamber and sequential advancement of pre-ignition and backfire into the intake manifold mainly under heavy load. The need to avoid pre-ignition/knocking phenomena is a serious consideration in all types of engines. If the burning velocity is increased and the combustion period is shortened, the occurrence of knock may be suppressed. Hydrogen, when added to gasoline, has been found to increase the burning velocity and therefore control the onset of knock; this might also be due the obstruction of radical production by hydrogen [8]. However it is the occurrence of pre-ignition that leads to backfire that has raised some important obstacles to the growth of hydrogen engines. A backfire occurs when the air-fuel charge is ignited during the intake stroke by heat sources before being ignited by the spark, resulting in combustion in the intake manifold. Hydrogen's minimum ignition energy is less than one tenth that of gasoline, which allows very small hot spots in the cylinder to ignite the hydrogen-air mixture during the intake stroke and flame to backfire into the intake system. Lubricant deposits, or the spark-plug electrodes, rather than the residual gas itself, are thought to initiate backfire [3, 19]. Hydrogen's small quenching distance also means that a hydrogen flame can more readily get past a nearly closed intake valve.

Table 1. Properties of Hydrogen and Other Fuels.

Parameter	Hydrogen	Methane	Gasoline
Density [kg/m^3]	0.09 (0 °C) 71 (-253 °C)	0.72 (0 °C) 423 (-162 °C)	730–780 5.1 (vapour)
Stoichiometry [kg_{Air}/kg_{Fuel}]	34.3	17.2	14.7
Lower Heating Value [MJ/kg]	120	50	43.5
Lower Heating Value at λ=1 [MJ/kg]	3.40	2.72	2.83
Boiling Temperature [°C]	-253	-162	25–215
Ignition Limits [Volume%, λ]	4–75, 0.15–10	5.3–15, 0.7–2.1	1.0–7.6, 0.4–1.4
Minimum Ignition Energy at λ=1 [mJ]	0.02	0.29	0.24
Autoignition Temperature [°C]	585	540	350
Research Octane Number	≥130	≥120	90–100
Kinematic Viscosity [m^2/s]	110×10^{-6}	17.2×10^{-6}	1.18×10^{-6}
Thermal Conductivity [W/m K]	182.0×10^{-3}	34.0×10^{-3}	11.2×10^{-3}
Diffusion Coefficient in Air [m^2/s]	6.1×10^{-5}	1.6×10^{-5}	0.5×10^{-5}
Quenching Distance [mm]	0.64	2.03	2.0
Laminar Flame Speed at λ=1 [m/s]	2.0	0.4	0.4–0.6

A general review of the research done on hydrogen as a fuel for automotive applications up to the mid 90's has been given by Norbeck *et al.* [20]. More recent reviews have been published by White *et al.* [21] and Verhelst *et al.* [22–23]. However, none of these have looked into both Spark Ignition (SI) and Homogeneous Charge Compression Ignition (HCCI), or Controlled Auto-Ignition (CAI), concepts. The following sections aim to provide an overview of both these combustion systems when used with hydrogen because both form an integral part of the current publication.

Spark Ignition: Hydrogen engines require a variety of parameters to be adjusted for satisfactory operation. Spark advance must be reset to suit the high flame speed of hydrogen; typically ignition must be retarded by up to 40° Crank Angle (CA) in comparison with gasoline at similar operating points. Additionally, as mentioned above, the wide flammability limits of hydrogen make it very prone to pre-ignition which along with knocking is one of its most discussed and controversial characteristics. The reason of such 'uncontrolled' autoignition issues seems to de dependent on load. One could argue that a fuel with such a high Research Octane Number (RON ≥ 130) should not show tendency to knock but hydrogen does not fit well into the normal definitions of octane number. It has a very high RON and a low MON (Motor Octane Number) [24]. MON is a better measure of how the fuel behaves under load because MON testing uses a similar test engine to that used in RON testing, but with a preheated fuel mixture, a higher engine speed and variable ignition timing to further stress the fuel's knock resistance. Typically, the MON of a modern gasoline is about 8–10 points lower than the RON. It can be said that hydrogen, with a much lower MON than RON, has a relatively low knock resistance in practice due to its very low ignition energy (primarily due to its low dissociation energy) and very high flame speed [24]. For example, Li and Karim [25] found that the knock-free operational region tends to narrow significantly with increasing compression ratio and/or intake temperature. It has also been documented that knocking of hydrogen is dependent on equivalence ratio and it is not due to end gas reaction [13].

Another issue of interest in hydrogen engines is that NO_X emissions from stoichiometric combustion of pure hydrogen, or from mixtures of hydrogen with natural gas or gasoline, are comparable, if not higher, to those from gasoline or natural gas engines (typically 2000–4000 ppm). However, it is possible to burn hydrogen in much leaner/cooler flames than gasoline or natural gas allows to, *i.e.* with Air-to-Fuel Ratio (AFR) greater than the stoichiometric one or, differently, for $\lambda=AFR/AFR_{stoic}>1$. This leads to relatively low NO_X emissions, especially for $\lambda>2.5–4.0$ [26–34]. Exhaust gas recirculation (EGR) can also be used to control the combustion duration, knocking and NO_X emissions in SI hydrogen engines [13, 35–40].

Particularly due to pre-ignition/backfire and NO_X-related problems, injection systems and mixture preparation strategies for hydrogen engines have attracted a lot of attention. However, no commercial injectors have been fully developed yet specifically for hydrogen engines because much larger volumes of fuel must be injected per stroke due to the very low density of hydrogen. Additionally, hydrogen's low lubricity leads to severe problems with the durability of injectors that have been originally designed for common fuels. Nevertheless, an appropriately designed electronically-controlled system can be adopted for engine operation with both hydrogen and compressed natural gas without any major alteration to the hardware of the system [41–42], particularly for research and demonstration purposes. Therefore, commercially available natural-gas injectors are generally being used nowadays as the baseline design for hydrogen injectors. Lee *et al.* [3, 19] reported that an intake port injection system of hydrogen could be easily adopted on a conventional SI engine with simple modifications, in contrast to in-cylinder high-pressure injection systems. Therefore, Port Fuel Injection (PFI) systems have been far more popular than Direct Injection (DI) systems, mainly due to their simplicity and relative ease of use as plug-on systems to standard SI engines [6–7, 43–44]. However, with PFI systems, main problems to overcome are backfire, air displacement and low calorific value of the inducted charge. A commonly used strategy to prevent backfire in PFI hydrogen engines is to retard the injection such that the end of injection is timed to occur just prior to intake valve closure. This enables hot residual gases to be cooled by fresh air [13]. Additionally, by keeping $\lambda>2$, backfiring can be generally eliminated [45]. However, mixtures of hydrogen and air formed by PFI typically have about 18% lower calorific value at stoichiometric conditions than gasoline mixtures which leads to a substantial power deficit and the need for supercharging [46–47].

Therefore, with regards to air displacement, energy density and power output, adoption of hydrogen DI systems is a better way forward [22]. In this case, the fuel is normally injected when the intake valves have already closed, therefore backfire is not an issue even at higher loads and, thus, richer engine operation can be achieved. Guo *et al.* [48] used a DI system to improve jet penetration and mixture formation and showed that backfire, pre-ignition and knock could all be controlled. On the other hand, PFI engines retain still all the advantages related to improved mixture homogeneity due to longer mixing times, extended lean operation, lower cyclic variability, lower NO_X production at part load and better efficiency. For example, Meier *et al.* [49] found that backfiring did not occur with internal mixture formation but the lean limit of operation was better with external mixture formation ($\lambda=4$ for PFI in comparison to $\lambda=3$ for DI). Yi *et al.* [50] discussed the development of a hydrogen DI system and concluded that this led to enhanced volumetric efficiency at high load and to higher level of engine output, but to higher level of NO_X at stoichiometry as well.

Although various technical problems of hydrogen SI engines have been tackled and solved in an empirical manner, very little work has been published on diagnostics of hydrogen combustion in optical engine designs. Heywood and Vilchis [51] were probably the first to use schlieren imaging to compare propane and hydrogen combustion in an optical SI engine. They showed that the propane and hydrogen flames fell in different turbulent flame regimes because the hydrogen turbulent flame thickness was about one third to one quarter that of propane, whilst the speed of burning was much faster that that of propane. Meier *et al.* [52] used Raman scattering in a DI hydrogen SI engine and reported that the quality of mixing was not affected by

injection timing which could be attributed to the high diffusivity of hydrogen. Rayleigh scattering and schlieren imaging have shown that high injection pressures may lead to hydrogen concentrations beyond the ignitability limit [53]. Meier *et al.* [49] used a schlieren system to visualise hydrogen-air mixture formation in an SI engine and calculated that the flame speeds obtained with internal mixture formation were significantly higher than those with external mixture formation. Laser Induced Fluorescence (LIF) techniques have been recently developed for the study of mixture formation in hydrogen engines, particularly with DI systems [54–55]. Additionally, recent studies involving flame chemiluminescence in DI hydrogen engines by White [56] (optical engine), as well as Wallner *et al.* [57–58] (endoscope), have illustrated the benefits of higher injection pressures and specific injector nozzle designs with respect to mixture formation and NO_X emissions.

Controlled Autoignition: SI gasoline and Compression Ignition (CI) Diesel engines have recently been accompanied by CAI or HCCI engines. CAI/HCCI engines may be considered as hybrids of SI and CI engines because these use premixed charge as SI engines do, but the charge is forced to autoignite by compression as in CI engines. Autoignition occurs simultaneously at multiple points across the cylinder, resulting in very fast combustion and enabling all the heat to be released within a short time space [59].

Although HCCI has attracted significant attention by various research groups during the last decade, there are still several difficulties in applying this mode of combustion to current engine designs over a wide range of operating conditions because several fundamental questions still need to be answered with respect to the in-cylinder physics of this combustion mode [60]. However, it is already well-known that large amounts of residual-gas recirculation and/or air-preheating are essential to achieve HCCI combustion [61–64]. The combination of fast heat release and the use of a lean charge, gives close to constant volume combustion with low peak gas temperatures leading to reduced heat transfer losses through the cylinder. The main benefits of HCCI combustion are very low NO_X emissions and overall improvements in fuel economy/efficiency [65].

Since HCCI engines operate on controlled autoignition of fuels, the use of high compression ratios has been deemed essential. Combustion chamber geometry has also been reported as quite important [66]. Conventional SI engine designs are typically limited to a compression ratio of approximately 11:1 (the latter mainly for DISI engines that benefit from the effects of increased charge cooling), therefore quite sophisticated systems are required to enable HCCI on current engine geometries. For example, use of fully variable valve timing systems with fully flexible valve timing strategies are needed to promote various levels of non-cooled internal EGR and also effectively induce variable compression ratios over a range of engine operating conditions.

Although HCCI engines have been reported to be very fuel flexible from the outset [67] and significant HCCI literature already exists on a variety of fuels [68], there is still very little knowledge on the use of hydrogen as the only fuel in HCCI engines. Theoretically, an HCCI engine running on hydrogen could lead not only to zero local emission of CO_2, CO, UHC and PM, but to near zero emission of NO_X as well due to the low temperature reactions involved with HCCI combustion. Thus, a successful hydrogen HCCI combustion system could result in a highly efficient and truly emission-free engine, potentially able to challenge alternative propulsion power plants and, for example, perhaps serve to bridge the gap between internal combustion engines and fuel cells.

The autoignition temperature and diffusivity of hydrogen are both higher than those of gasoline or mixtures of n-heptane/iso-octane in air, implying a very different mixing and autoignition mechanism. Naber and Siebers [69] investigated the autoignition of hydrogen in a constant-volume combustion chamber under simulated engine conditions with large amounts of dilution and showed that reasonably short ignition delays were obtained for ambient gas temperatures greater than 1120 K and for O_2 concentrations in the range 5–21%. A five-fold decrease in ignition delay was observed for a 10% increase in ambient gas temperature. The dependence of ignition delay on ambient pressure was small. Their results suggested that a hydrogen autoignition engine could meet ultra low emission standards without exhaust gas after-treatment by using intake charge dilution techniques. Noda and Foster [70] made a numerical study on the effect of inhomogeneities on hydrogen HCCI combustion, concluding that the intake gas temperature was more dominant on autoignition timing than the AFR was. Lu *et al.* [71] used chemical kinetics modelling to show that some chemical species, including OH, can significantly change the pace of autoignition; adding these species to the mixture prior to ignition changed the initiation of the chain reactions and significantly reduced the ignition delay.

In real engines, hydrogen has been mainly researched as an 'additive' fuel to HCCI combustion systems, *e.g.* from a reformer or in combination with DiMethyl-Ether (DME). In such studies, better control of the timing of autoignition and improved thermal efficiency have been reported [72–75]. Yap *et al.* [76] studied hydrogen addition to a natural-gas HCCI engine using modelling and experiments and found a reduction in the intake temperature required for HCCI operation, presumably due to the higher diffusivity and better mixing of hydrogen with air. The first demonstration of pure hydrogen HCCI combustion was published by researchers at Lund [77]. They studied hydrogen HCCI in a single-cylinder thermal engine of large capacity (1.6 lt) at high compression ratios (typically 15:1–20:1) using external mixture preparation and air preheating. They found that intake temperatures of the order 80–160 °C were needed for successful operation in the range λ=4–6 for 800–1600 RPM. More recent work published in [78] presented hydrogen HCCI measurements from a

thermal engine of 0.825 lt equipped with a PFI system within a similar operation range to that identified at Lund. These authors also demonstrated negligible levels of NO_X, CO and PM in comparison to Diesel operation of the same engine.

Most published results on HCCI combustion are mainly based on parametric studies. Results from optical engines are rather limited in the literature and focused on hydrocarbon fuels using combustion imaging techniques and LIF measurements [79–83]. Spectroscopic studies of major species related to the autoignition process can be very useful to clarify the nature of the reactions involved. Hultqvist *et al.* [82] showed cool-flame emission spectra from iso-octane/n-heptane HCCI combustion and discussed that these spectra originated from the presence of formaldehyde (HCHO). LIF studies have shown how HCHO and OH species are present within the 'cool' flame period and subsequent 'hot' combustion [84–86]. The absence of carbon atoms, and thus HCHO, from the in-cylinder mixture of a hydrogen HCCI engine means that a totally different mechanism of autoignition is in operation and that OH generation would be very different from that of hydrocarbon fuels. For example, the presence and amount of H_2O_2 (typical species found in the oxidation mechanism of many common fuels, as well as in that of hydrogen) has been found to affect HCCI combustion [87]. In view of such differences, several studies of hydrogen HCCI have been performed by various types of modelling approaches, including multi-zone models, chemical kinetics and Direct Numerical Simulation (DNS) [89–90].

As far as optical studies of hydrogen autoignition are concerned, Markides and Mastorakos [91] studied recently the mechanism of hydrogen autoignition in a turbulent co-flow of heated air by OH chemiluminscence imaging. They concluded that autoignition was relatively insensitive to changes in hydrogen dilution and that there was a delaying effect of turbulence on autoignition. Apart from such type of rig work, there are currently no studies in background literature that discuss explicitly hydrogen autoignition in optical research engines. This is one of the gaps in the literature that the current paper wishes to fill; specific objectives are summarised in the following section.

GOALS AND CURRENT CONTRIBUTION

Most recent work on hydrogen engines has mainly focused on spark ignition. The effects of spark advance and EGR have been largely investigated in order to control combustion, emissions and extend the lean limit. Very little work has, however, been done on optical engines [56] and there is still great need for high resolution combustion images to understand the effect of engine operation parameters on hydrogen's thermodynamic performance, especially in direct comparison with common fuels like gasoline. As far HCCI is concerned, at present there is very scarce literature on the subject of hydrogen [77–78] and to the best of the author's knowledge no study has presented and discussed in-cylinder combustion images of pure hydrogen HCCI. Furthermore, the engines that have been adopted for hydrogen HCCI studies have had high compression ratios, typically greater than 15:1. Therefore, autoignition of the fuel was obtained with relatively mild intake air preheating, typically in the range 100–150 °C.

The present work aims to provide and discuss probably the first ever set of hydrogen combustion data in the literature from the same optical engine in both SI and HCCI modes of operation and to specifically characterise hydrogen combustion by:

- Sweeping a broad set of engine operating conditions with hydrogen fuel (AFR, intake temperature and internal EGR) and comparing the results against those obtained with conventional fuels, namely gasoline for SI combustion and heptane for HCCI operation.

- Studying flame imaging data with both DI and PFI mixture formation strategies and identifying key mechanisms of in-cylinder combustion phenomena linked to these strategies when hydrogen is used in direct comparison to other fuels.

- Illustrating means by which steady HCCI operation on sole hydrogen can be achieved in an engine of typical pentroof geometry and relatively low compression ratio.

- Examining the effect of both single and double hydrogen injection strategies per cycle for DI operation on both SI and HCCI modes of engine combustion.

It was the authors' intention from the outset to publish this work as one entity, rather than in a series of individual papers focused on either SI or HCCI combustion with either PFI or DI operation and in either thermal or optical mode. It is believed that the present contribution to much-needed hydrogen engine combustion data in the literature is rather unique. It needs to be pointed out though that the current account is by no means complete. Analysis of the acquired data is ongoing and will be expanded in forthcoming publications.

EXPERIMENTAL ARRANGEMENT

OPTICAL ENGINE

Engine Geometry: The engine used in this study was a single-cylinder optical research engine designed and built at University College London (UCL) [92]. The bore of the engine was 89 mm and the stroke was 79 mm. Geometrical properties of the engine, along with other specifications and characteristics are summarised in Table 2.

Table 2. Engine Specifications.

Engine Type	4-Stroke, Single-Cylinder Optical
Engine Head	4-Valve Pentroof, Prototype V8
Piston shape	Flat
Bore [mm] × Stroke [mm]	89 × 79
Optical Bore [mm]	66
Displacement [cm^3]	498
Injection System	PFI Single-Hole, DI Multi-Hole

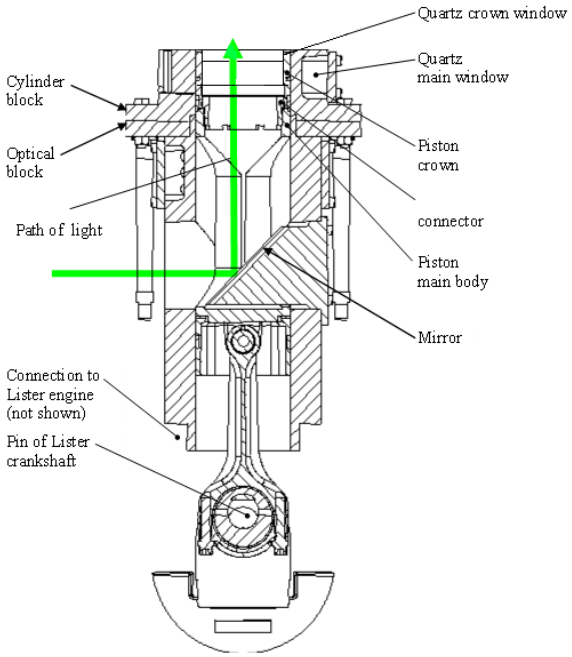

Figure 1. Optical Engine Section (Head not Shown).

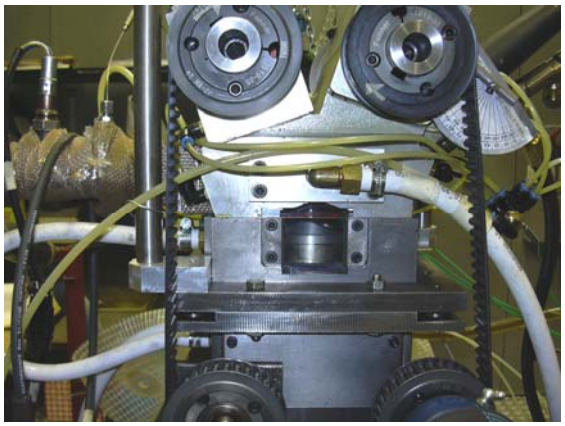

Figure 2. Optical Engine.

Figure 1 shows a schematic section of the engine. The engine block was attached to a Lister-Petter Diesel crankcase allowing a maximum running speed of 2000 Revolutions Per Minute (RPM). A hollow Bowditch piston allowed for a 45° stationary mirror to be fitted inside the block in order to gain optical access to the combustion chamber through a quartz piston crown. The engine design also accommodated a pentroof window and side full stroke window for optical access through the liner. However, it was only the piston optical crown arrangement that was retained for the current study due to uncertainties involved in the thermal stressing of the engine with hydrogen operation, especially in HCCI mode. All the quartz components of the engine could be replaced with metal blanks in order to run the engine in fully thermodynamic mode when investigating unknown firing conditions for this engine or for prolonged mapping work. Figure 2 shows a picture of the optical engine. It should be noted here that with such a configuration there was no lubrication provided to the top end of the engine therefore self-lubricating materials had to be used for any working components between liner and piston. For the extreme conditions employed in the current study, after trying different type and grades of Peak, it has been found that Torlon was the most suitable material, mainly due to its resistance to high temperatures and aggressive environments.

Fuel Supply Systems: The engine head was a prototype of 4-valve pentroof type, with a central spark plug and a side DI system arrangement. In order to study operating conditions with both hydrogen and gasoline within the bounds of the current work, the engine was converted to accommodate a fully flexible fuelling system, capable of both PFI and DI of both liquid and gaseous fuels. A view of the injection system showing all the injectors used is illustrated in Figure 3. Three injectors were fitted on the engine, two on the intake ports allowing for simultaneous injection of liquid and gas fuels (one on either intake port) and one in-cylinder for DI engine operation. Hydrogen gas was supplied straight off a pressurized bottle by means of a pressure regulator, typically set up to 100 bar for DI and 4 bar for PFI work. The whole fuel supply system comprised the aforementioned regulator, a back-flash arrestor, a micrometric in-line filter and a mass-flow controller (Bronkhorst F-203AC). The latter was connected via a serial cable to a computer in order to monitor and control the fuel flow to the injector in real time. Liquid fuels were supplied through a fully adjustable pneumatic pump (connected to a compressed air line) capable of a maximum pressure up to 150 bar.

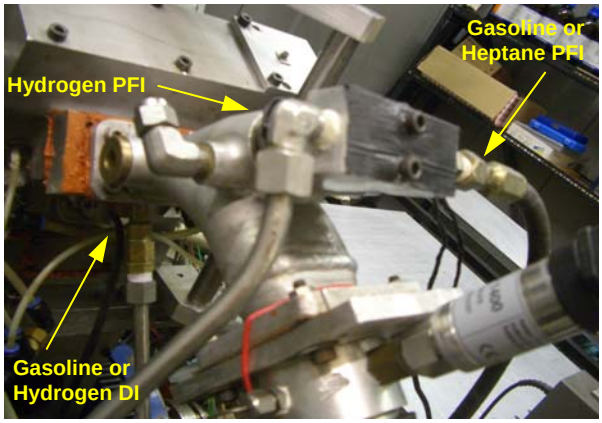

Figure 3. Injection System Setup.

Fuel Injectors: A standard Bosch single-hole fuel injector was used for the PFI gasoline system. Hydrogen was injected in the intake port using a Keihin KN3-2 gas injector. Selection of the injector for the DI fuelling system was not trivial. The engine head had been designed to operate with a side pressure-swirl atomizer at 45° inclination below the intake valves. One of the requirements of the DI system for the current work was to allow flexibility for use with both liquids and gases. The pressure swirl atomizer was deemed inadequate for this and a multi-hole injector was finally selected. This decision was backed by some previous work in the literature [93]. The selected injector nozzle had a 6-hole arrangement that consisted essentially of two groups of 3 asymmetric holes of 0.5 mm outer diameter each, originally designed for a spray-guided DI gasoline combustion system for both stratified and homogeneous engine operation, with vertically mounted injector in close-spacing arrangement with the spark plug. This was the most cost-effective choice able to cope with the high flow-rate requirements needed for hydrogen. It must be pointed out here that it was only the short running periods involved with optical engine operation that made it possible to safely adopt such a solution, because lack of lubrication would not allow the injector to live long due to seizing problems. The choice, although at first quite daring, eventually proved to be successful enough. The position of the injector and its nominal spray pattern with respect to the combustion chamber are shown in Figure 4. Due to the asymmetry of the nozzle-hole pattern, it was after several tests of engine combustion stability that decision was made to adopt the orientation with the two sets of plumes pointing upwards towards the pent-roof as shown in Figure 4. No more details can be disclosed with regards to the exact type and geometry of this injector.

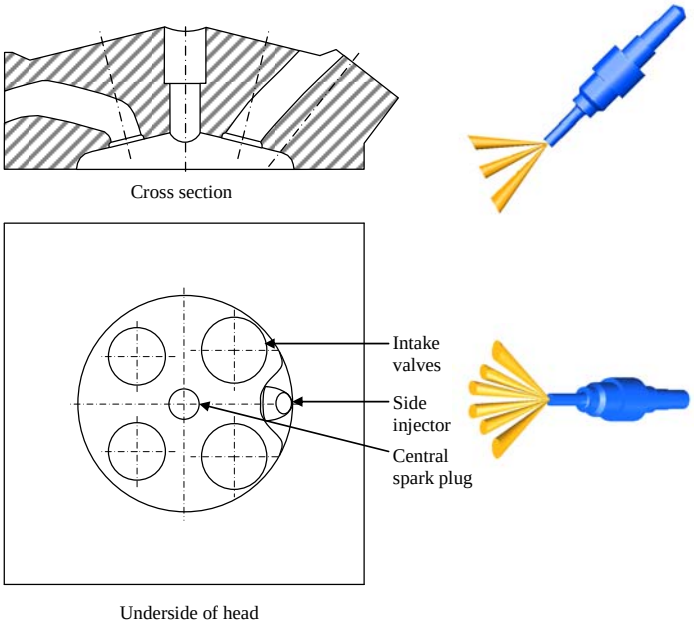

Figure 4. Engine Head Geometry and Orientation of Injector with Nominal Spray Pattern.

OPERATING CONDITIONS

For the results that will be reported in this paper, the engine was operated either in DI or PFI mode with gasoline or hydrogen in SI combustion mode. HCCI was enabled with simultaneous PFI of heptane and DI of hydrogen or with sole DI hydrogen, using 4 bar injection pressure for the PFI systems and 70 or 100 bar for DI, with various timings of Start of Injection (SOI) that will be presented and discussed later. It must be pointed out that higher injection pressures would be ideal for gas DI in order to shorten the injection pulses whilst providing the engine with the required mass-flow within the appropriate time window during the thermodynamic cycle; however, the selected pressure was the highest permitted by the gas mass-flow controller. The engine speed was set to 1000 RPM. Both the engine head and liner were heated to 85 °C to represent typical warm running engine conditions. The load was set by the throttle to either 0.5 or 1.0 bar intake manifold pressure under SI combustion mode to enable typical part-load and full-load engine operation. The intake pressure was monitored by a Druck PMP1400 pressure transducer. Particular care had to be taken when running the optical engine on hydrogen at full load close to stoichiometry due to the large peak in-cylinder pressures achieved. In HCCI mode the engine was run always unthrottled.

Ignition System: The ignition system was of standard coil and driver type. The dwell time was set to 3 ms to limit the electronic noise on the data acquisition system. The spark plug was a Bosch Platinum with quadruple electrode, the orientation of which within the combustion chamber was established by the thread pattern of the plug. Initial tests were carried out to identify suitable ignition timings by mapping the engine and establishing the Minimum spark advance for Best Torque (MBT) for each fuel used and injection system. Typical MBT timings were in the range of 30–40° CA before compression TDC for gasoline and 8–15° for hydrogen. Ignition timings will be discussed further in the results section. Crank angle timings with respect to ignition timing will be referred to as °CA After Ignition Timing (AIT).

Air Pre-Heating and Internal EGR: For HCCI operation the engine was fitted with an air pre-heating system of 2.3 kW that could control the intake air temperature in the range 50–400 °C. Such a wide range of temperatures was required to enable HCCI with a range of different fuels and AFRs because of the low compression ratio of the optical engine (7.5:1). As it will be further discussed in the results section, a necessary step to achieve hydrogen HCCI was to adapt the valve timing, aiming to trap hot residual gases in order to further increase in-cylinder temperature and retain chemical species. The strategy employed was a two-stage reduction of the overlap by means of an advanced Intake Valve Closing (IVC) time and a retarded Exhaust Valves Opening (EVO) time which eventually led to a small recompression at intake TDC, as clearly visible in the motoring pressure trace shown in Figure 5.

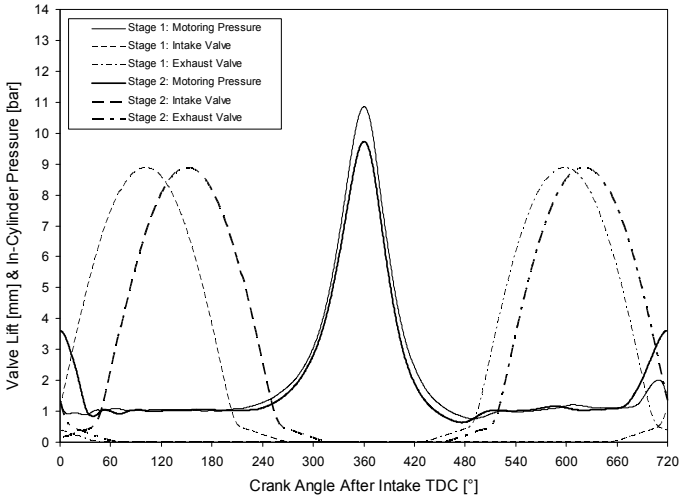

Figure 5. Valve Timings and Motoring Pressure.

The results of the current publication will be presented according to their chronological order. This decision was made in order to highlight how gradual progress was made to finally achieve pure hydrogen HCCI. Figure 5 also shows the two valve-timing strategies adopted towards the goal of sole hydrogen HCCI engine operation. The first stage (Stage 1, in Figure 5) enabled a reduced valve overlap in comparison to that of the nominal design, namely of 6.5° CA. This was used to operate the engine with SI hydrogen and gasoline, as well as to enable HCCI of heptane and mixtures of heptane and hydrogen. Although this approach proved to be a good starting point, it was found insufficient for operating the engine in pure hydrogen HCCI mode. The second stage (Stage 2 in Figure 2) aimed at further decreasing the valve overlap, namely switching from 6.5° CA positive to 20° CA negative. It also needs to be pointed out here that the valve timings were not dictated solely by the desired overlap, but also by volumetric efficiency requirements and, quite importantly, by the necessity to maintain a reasonable clearance between the quartz piston crown and the valves of the engine. Table 3 summarises the typical operating conditions adopted for this study. It should be noted that in this paper 0° CA corresponds to Intake Top Dead Centre (TDC) and crank angle will be mainly presented with respect to that as ° CA after intake TDC (ATDC).

Table 3. Operating Conditions.

Engine Speed	1000 RPM
Intake Pressure	0.5 and 1 bar
DI Pressure	70 and 100 bar
PFI Pressure	4 bar
Engine Temperature	85 °C
Intake Temperature	20–400 °C
Valve Timings Stage 1 [° CA ATDC] Stage 2 [° CA ATDC]	 IVO 706, IVC 216, EVO 482, EVC 712 IVO 36, IVC 266, EVO 506, EVC 16

IMAGE AND DATA ACQUISITION

A high-speed CMOS camera (Photron APX-RS) was used throughout this study at a frame rate of 3 and 6 kHz, corresponding respectively to 2° and 1° CA between frames at 1000 RPM. This was possible with an image resolution of 640×480 pixels, giving an optical resolution of 260 μm per pixel. A 60 mm f2.8 Nikon lens was used. The camera memory allowed over 100 cycles of data with 50 frames per cycle to be acquired consecutively before data-download to a PC was necessary. It was nevertheless considered safer to fire the engine in optical mode only for 50 cycles each time to avoid excessive stresses on the quartz window, especially with HCCI. A water-cooled Kistler 601A pressure transducer was also used and pressure data were logged in batches of 50 cycles too. Synchronization of various control triggers for ignition, injection and camera was achieved using an optical encoder on the camshaft with a resolution of 1800 pulses per revolution. This was connected to an AVL Engine Timing Unit and a LABVIEW program was used for data acquisition at 0.4° CA resolution. Thermodynamic analysis was done on the pressure traces with MATLAB-based software to calculate rates of heat release and Mass Fraction Burned (MFB). Further details of the systems in [94, 95].

RESULTS AND DISCUSSION

SPARK IGNITION

Thermodynamic Data

The first step along this study was switching from gasoline to hydrogen SI in order to test the rig and acquire familiarity with the new fuel. Due to the optical nature of the work, the AFR investigated was mainly in the range λ=1.2–2.0 to provide enough luminosity for combustion images of adequate quality. It must be pointed out though that steady combustion could be achieved with much leaner AFR (*e.g.* λ=3). At the same time, load and fuelling had to be carefully adjusted to prevent damage to the optical components of the engine. This was done by matching higher engine load (intake pressure) with leaner AFR to limit peak in-cylinder pressures. The graph presented in Figure 6 shows the influence of AFR on combustion of gasoline and hydrogen with different injection modes; the load was set to 0.5 bar intake pressure, DI pressure to 70 bar for hydrogen and 100 bar for gasoline, SOI to 220° CA ATDC intake and spark ignition to 345° CA and 325° CA ATDC intake for gasoline and hydrogen, respectively. It is obvious that the AFR has a strong effect on combustion rate and in-cylinder pressure for hydrogen; as the richness of the mixture increases, higher in-cylinder pressure is achieved and the angle at which maximum pressure occurs moves towards TDC combustion or even earlier than that. Although the hydrogen spark advance corresponded to MBT only for λ=2.0 PFI, this was kept fixed for comparison with the other values of AFR tested and DI operation. It is evident that due to the very rapid combustion of the closer to

stoichiometry hydrogen mixtures, the spark advance would need re-adjustment in order to obtain peak pressure after TDC and thus achieve a more efficient work exchange during expansion. However, it was kept fixed to look into whether knocking would be observed for such a larger spark advance than MBT for the richer values of AFR, particularly with DI. The different combustion durations are due to the effect of AFR on laminar flame speed and, therefore, flame propagation [12]. By comparing DI and PFI at λ=2.0, it can be understood that the injection mode also plays a central role on the development of combustion. DI leads to higher peak pressure along with higher combustion rate. This difference can be explained by the disparity in the calorific value of the two in-cylinder mixtures. Externally formed hydrogen-air mixtures have been found to carry less energy because of air volume displaced by the hydrogen injection in the intake port [22]. Additionally, the inhomogeneity (or stratification) of the in-cylinder mixture brought about by close-valve DI may lead to some much richer spots than the average fuel concentration within the cylinder. These will burn proportionally quicker for hydrogen than they would for gasoline with similar degree of stratification, mainly due to the much higher laminar flame speed of hydrogen and wider flammability range.

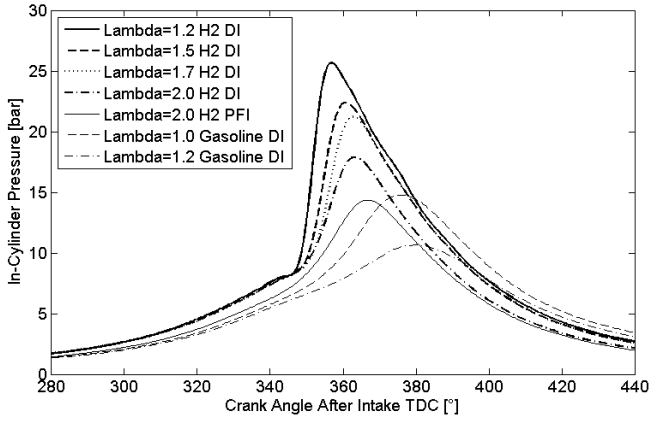

Figure 6. Effect of AFR on In-Cylinder Pressure for SI of Hydrogen, Gasoline (Part Load, Spark Advance 15° CA for Hydrogen, 35° CA for Gasoline).

Some of these trends are partly confirmed by previous work where pressure traces of DI and PFI stoichiometric hydrogen combustion have been compared to gasoline [11]. The behavior shown in Figure 6 at part load presents some analogies with the one documented in [11] at full load, 2000 RPM and stoichiometry, with a substantial difference between the pressure output of gasoline and hydrogen PFI. Stoichiometric gasoline in [11] achieved higher peak pressure than hydrogen PFI, opposed to the trend shown in Figure 6. A sensible explanation for this might be the very large volume displaced by the stoichiometric air demand of hydrogen at the higher RPM, in synergy with the higher compression ratio adopted, which gasoline might have been more sensitive to with the spark advance used. Furthermore, another difference between pressure data presented here and data in the literature, is that a closed-valve hydrogen DI strategy with SOI=220° CA ATDC and a spark advance of about 10° CA (*i.e.* similar to the values used in the present study) has been documented in Wimmer *et al.* [12] to lead to a gentler pressure raise in the early stages of combustion for λ=1.0 in comparison to pressure data shown in Figure 6 for hydrogen DI at λ=1.2. This might be associated with the difference in engine speeds, 1000 RPM in the current study, 2000 RPM in [12]. It also useful to compare in-cylinder pressure data for different fuels at the same air excess ratio and with the same injection mode. Figure 6 shows pressure traces for DI gasoline and hydrogen at λ=1.2. Although the fixed spark advance employed was over-advanced for hydrogen DI in comparison to MBT at this operating point, no knocking was observed on the pressure traces and hydrogen was found to produce more than twice as much peak in-cylinder pressure that gasoline did and at a timing about 35° CA earlier than gasoline. It must also be noted that the λ=1.2 chosen for this comparison fell well within the flammability window of hydrogen, whereas this was at the boundaries of misfire for gasoline, contributing further to the large gap in combustion rates between hydrogen and gasoline. The raised pressure curve observed for hydrogen during the compression stroke is related to the closed-valve DI of the gas, whose volume, unlike liquid fuels, cannot be neglected and creates the gap between the two pressure curves. This has also been discussed in [11]. Figure 7 presents the respective MFB traces for each case of Figure 6. The much quicker combustion of the richer hydrogen mixtures is confirmed. At λ=1.2 combustion completion is reached at just 11° CA AIT, as opposed to 18° CA for at λ=1.7. The influence of the internal EGR induced by the selected valve overlap (Stage 1) must be taken into consideration when looking at these data; trapping extra residual gases certainly imposed a penalty on the rate of heat release. This can explain the relatively slow combustion rate of gasoline observed at this running condition.

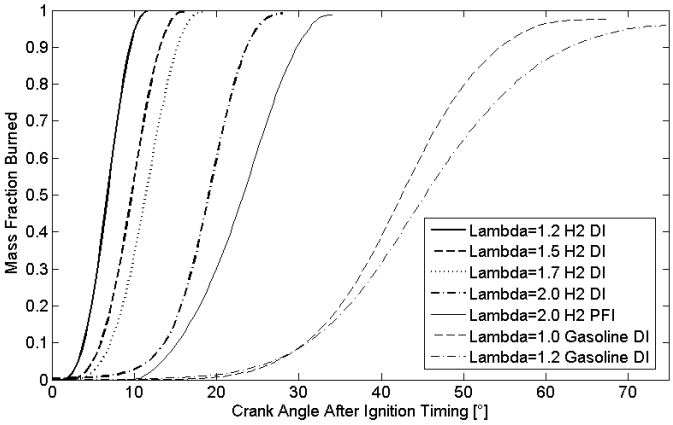

Figure 7. Effect of AFR on Mass Fraction Burned for SI of Hydrogen, Gasoline (Part Load, Spark Advance 15° CA for Hydrogen, 35° CA for Gasoline).

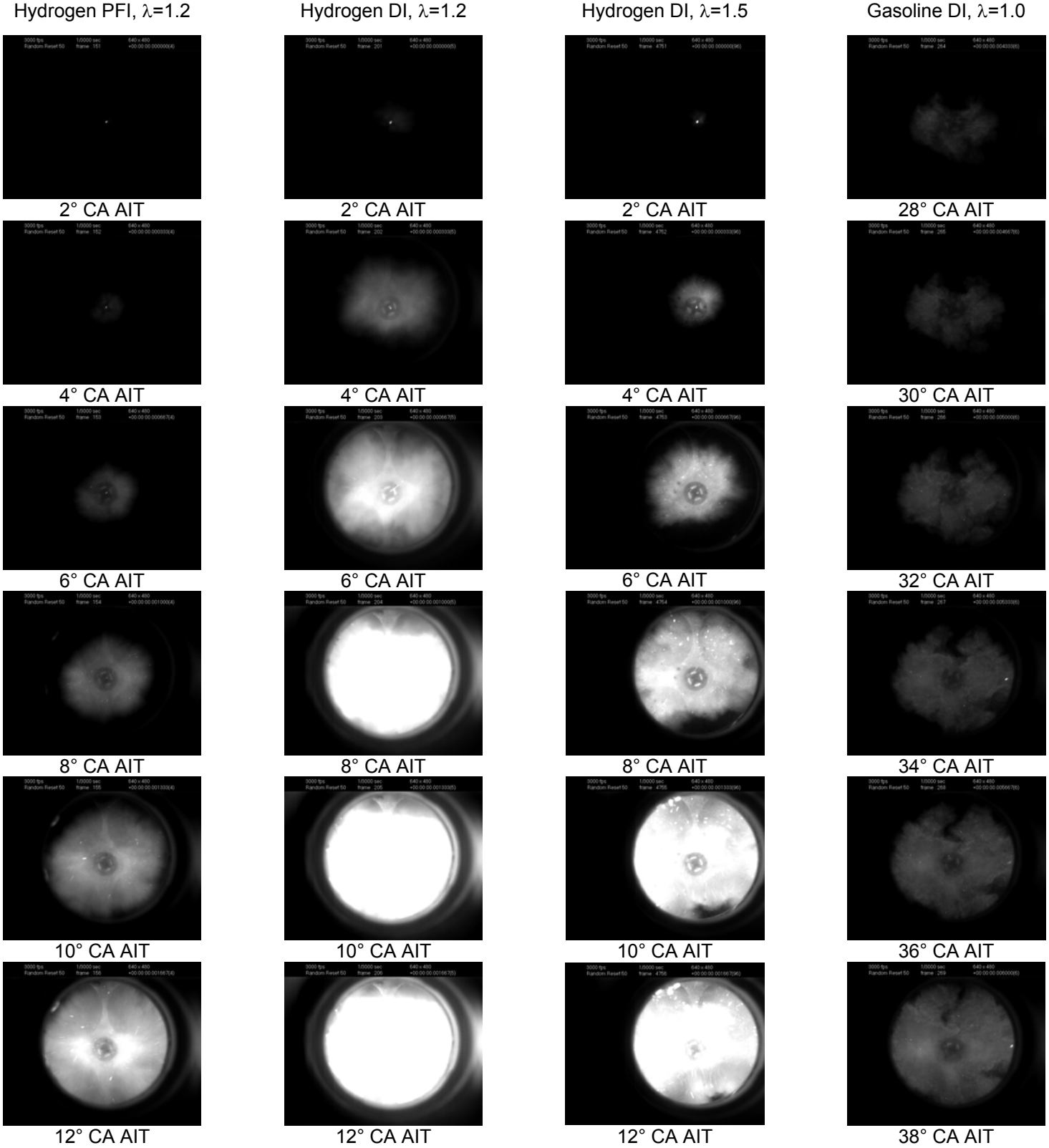

Figure 8. SI Flame Development: Part Load, Spark Advance 15° CA for Hydrogen, 35° CA for Gasoline (Intake Valves at the Top, Exhaust Valves at the Bottom).

High-Speed Imaging

The trends discussed throughout the analysis of the thermodynamic data were also reflected by the flame images acquired. Figure 8 presents typical sets of crank-angle resolved flame development images for gasoline DI, as well as hydrogen DI and PFI at part load (0.5 bar intake pressure) with different air excess ratios. The injection timing was set to SOI=220° CA ATDC for DI regardless of fuel (*i.e.* very close to the IVC timing, as presented earlier in Table 3 and Figure 5), 360° CA ATDC for PFI gasoline (*i.e.* injection against the hot closed intake valves at compression TDC) and 0° CA ATDC for PFI hydrogen (*i.e.* against open intake valves at intake TDC). These images have not been post-processed in any fashion and the luminosity shown is the actual raw flame chemiluminescence of the fuels as recorded by the camera without the need of an image intensifier.

Firstly it is interesting to underline the diverse behaviour of hydrogen according to the injection mode selected. As already demonstrated through thermodynamic data, hydrogen PFI shows slower combustion when compared with hydrogen DI. Namely, with the latter, the flame fills the optical piston crown and achieves partial saturation at about 6° CA AIT, as opposed to PFI where similar flame behaviour is achieved at 12° CA AIT. This could be explained once again by the different grades of in-cylinder mixture homogeneity and to the difference in calorific value between the mixtures depending upon where these were formed. A comparison between hydrogen's DI flame images in the range 4–8° CA AIT for λ=1.2 and λ=1.5 demonstrates that there is about 2° CA difference in reaching roughly the same flame radius for the leaner case of the two. Despite this, the hydrogen flame always shows a relatively circular shape. A fairly spherical flame growth was generally expected for a well-mixed hydrogen-air charge, especially considering the Lewis number of this fuel. From this it can be speculated that the chosen injection timing (SOI=220° CA ATDC) allowed enough time for the injected gas to mix and settle before ignition. In order to further understand timings related with injection timing, mixing and ignition of hydrogen, it is worth mentioning that at the actual injection pressure used (70 bar) and engine load (0.5 bar intake pressure), the DI system required a pulse-width ranging from 4 to 6 ms, to fulfil fuel requirements at the air excess ratios presented. At 1000 RPM, 6 ms correspond to 36° CA which leaves 89° CA for hydrogen to mix and lose most of its initial jet momentum before ignition. Similar circular flame development has been observed by White [56] at 1200 RPM with a similar injection timing to that used in the present study (albeit the different injection pressure employed and the different injection system). It should also be noted for completeness that the frame rate of the camera was specifically selected to capture images of sufficient luminosity at the lean fuelling condition shown. This could have contributed to the blurred appearance of the flame due the very fast flame growth of hydrogen.

It is also interesting to compare the images of combustion with DI of gasoline at stoichiometry (λ=1.0) with those of hydrogen at the richest AFR tested in this study (λ=1.2). The main feature is certainly the difference observed in flame speed between the two fuels. Gasoline flames were at the earliest visible at about 20° CA AIT, in comparison to just 1–2° CA AIT for hydrogen. The sharper look of gasoline flames is related to the lower flame speed which enabled the camera system to 'freeze' the flame motion better than in the case of hydrogen. Furthermore, the structure of the gasoline flame front demonstrates clearly its interaction with the flow field and turbulent eddies. Gasoline also appears to follow a different path of development, namely starting from the exhaust side and gradually moving back toward the intake side and gradually filling the full optical crown. This might suggest that, either gasoline is sensitive to the temperature gradient across the bore, or that the mean tumble motion imposed by the pentroof geometry carries the flame towards the exhaust side first. Alternatively, this behaviour might be related to the fuel concentration field, but currently no information exists on the in-cylinder flow field or fuel concentration to support one of these more against the other. Hydrogen seems to be less sensitive to any of these parameters, on the assumption that its mixing with air was far better than that of gasoline, *i.e.* the temperature gradient between intake and exhaust side, as well as the presence of any large scale motion due to tumble does not make hydrogen depart from a spherical growth.

HOMOGENOUS CHARGE COMPRESSION IGNITION

Thermodynamic Data

Heptane: Once the experiments on spark ignition were completed and enough familiarity with hydrogen set up was acquired, the following step was to switch from SI to HCCI. For the first batch of experiments n-heptane was adopted, due to its low octane number, mainly to gain control of the new combustion mode and understand the engine's behavior in response to new set of parameters. As extensively acknowledged by previous work, the most common fashion of enabling compression ignition is by means of intake air pre-heating, especially if one needs to compensate for the low compression ratio of an engine [61–62]. For the aim of this study, the intake air temperature was raised up to 200° C in order to enable HCCI combustion of the leaner heptane mixtures studied. For safety reasons and in order not to over-stress the optical engine, spark ignition appeared to be, regardless of injection mode, the best way to start firing the engine. Then transition to HCCI was enabled by switching the air-preheating system gradually on and disabling the spark.

Figure 9 shows in-cylinder pressure traces of heptane in PFI mode at various values of AFR, with SOI at 360° CA ATDC (*i.e.* injection against the hot closed intake valves injection at compression TDC) and intake air temperature fixed at 180 °C. In fact, it was found that

autoignition of heptane was possible around 140 °C but most of the test points were set to 180 °C and 200 °C intake air temperature in order to sustain reliably steady HCCI combustion. In Figure 9, the richest mixture of λ=1.4 is seen to start main combustion at about 5° CA ATDC and subsequently reach peak pressure in the next 7° CA. The leanest mixture of λ=2.0 exhibits retarded ignition, namely at 12° CA ATDC and a gentler pressure rise, reaching peak pressure at 22° CA ATDC. The period of cool flame that is characteristic of heptane's autoignition mechanism is visible as a small pressure increase at the end of compression. This period of combustion can be manifested in one or two stages depending on the equivalence ratio of the mixture and this is largely acknowledged in background literature [65, 86]. The cool flame is due to heat release from formation energies of aldehydes, water and CO, as opposed to the main combustion event which seems to be dominated by oxidation of CO to form CO_2. It is believed that the transition between one and two stages of cool flame just before the main combustion event occurs at about λ=4 [65]. At conditions richer than λ=4, the reaction rate of the mixture becomes too high to observe the distinction between the second stage of cool flame and the main combustion event, leading essentially to one obvious stage of cool flame and thus a two-stage combustion mechanism. This two-stage characteristic behaviour appears in Figure 9 because fuelling was kept always richer than λ=4, namely in the range λ=1.4–2.0.

Figure 10 illustrates the heat release traces for the same conditions of Figure 9, *i.e.* at a fixed intake temperature of 180 °C for different values of λ. Then, for comparison, Figure 11 and Figure 12 present in-cylinder pressure traces and rates of heat release, respectively, for two different intake air temperatures at a fixed air excess ratio of λ=1.4. It is important to note the two distinctive stages of heat release mentioned earlier. The heat release traces in Figure 10 reveal clearly that the main combustion is affected more by the quality of the mixture (*i.e.* overall λ) than the cool flame which tends to be driven by temperature, as shown in Figures 11–12. The intake air temperature appears to have the strongest effect on ignition delay due to the fact that it affects the timing of cool flame development and thus indirectly drives the start of main combustion too. The above suggests that, when conditions impose a given AFR, *i.e.* fixed load, intake air temperature is an effective means by which it is possible to control the phasing of main combustion.

These data confirmed the expected trends of HCCI from background literature, *e.g.* [65], even in engines of low compression ratio, *e.g.* [64], and provided confidence in moving towards the next step of the study, *i.e.* introducing hydrogen into a reliable HCCI combustion system, as will be shown in the next section.

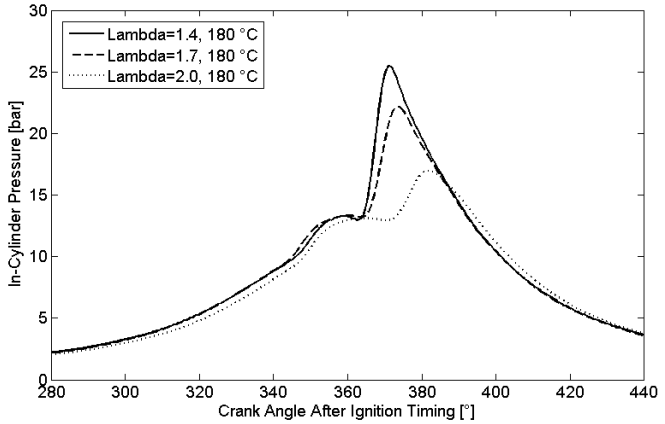

Figure 9. Effect of AFR on In-Cylinder Pressure for HCCI of Heptane (180 °C, PFI with SOI 360° CA ATDC).

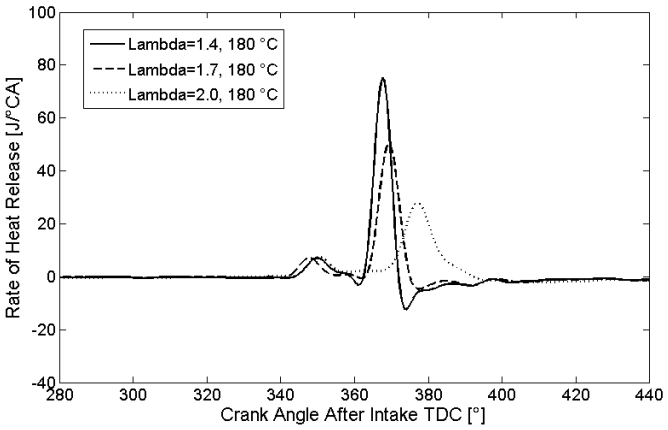

Figure 10. Effect of AFR on Rate of Heat Release for HCCI of Heptane (180 °C, PFI with SOI 360° CA ATDC).

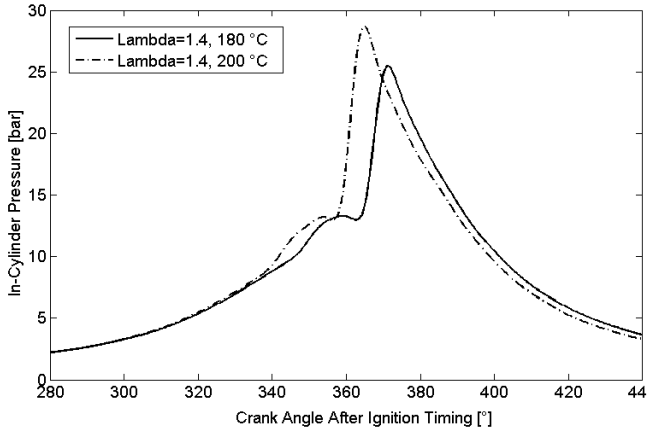

Figure 11. Effect of Intake Air Temperature on In-Cylinder Pressure for HCCI of Heptane (λ=1.4, PFI with SOI 360° CA ATDC).

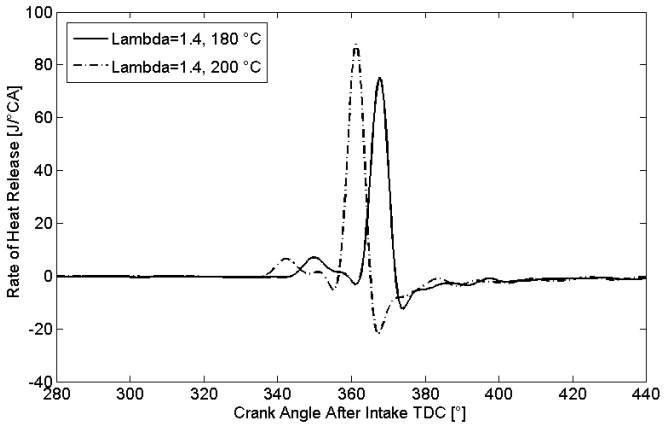

Figure 12. Effect of Intake Air Temperature on Rate of Heat Release for HCCI of Heptane (λ=1.4, PFI with SOI 360° CA ATDC).

Heptane/Hydrogen Mixtures: The next step involved introducing hydrogen injection into the heptane-fuelled HCCI engine. Although tests were initially carried out with PFI of both fuels, it was soon made clear that closed-valve DI of hydrogen was definitely more suitable for stable HCCI operation. This is because PFI hydrogen interfered with the intake air-heating system and did not permit tests with high intake temperature due to risks of dangerous backfire on the heating element in the intake. DI also prevented most other setbacks associated with PFI, such as air displacement, energy density and long injection pulse-widths. The strategy adopted was to use a so-called 'pilot injection' of heptane in the intake port at 360° CA ATDC (*i.e.* against the hot closed intake valves at compression TDC), followed by an in-cylinder closed-valve direct injection of hydrogen. The aim of this strategy was to allow certain flexibility in adjusting the overall octane number of the mixture, *i.e.* from pure heptane's minimum octane rating to pure hydrogen's maximum rating, by the relative independent injection durations of the two fuels under study.

The injection timing of hydrogen played a fundamental role in enabling sustainable HCCI combustion of mixtures of heptane and hydrogen. As commented in previous work, one of the features of hydrogen DI is the charge-cooling due to gas expansion, which is listed as one of the strengths of DI when associated with SI combustion since it helps prevent pre-ignition [11]. Recent computational work on hydrogen DI jets has discussed hydrogen's low inversion temperature, *i.e.* the point at which the Joule-Thompson coefficient equals zero [96]. For temperatures higher than the inversion temperature of a given gas, this coefficient is negative, and thus the temperature increases as the gas expands in a throttling process. In contrast to most common gases, hydrogen has a very low inversion temperature, namely 202 K at 1 bar and 125 K at 345 bar [97]. This means that hydrogen gas exiting from a pressurised tank initially heats, rather than cools. In the present study, hydrogen is injected into the cylinder at a colder temperature than that of the highly preheated in-cylinder air. This has an impact on the temperature of the in-cylinder charge which is difficult to estimate due to the coupling of several mechanisms linked to both the negative Joule-Thompson coefficient and hydrogen's much larger specific heat capacity on a kg basis than that of air. Obviously any cooling effect becomes a setback when the aim is in-cylinder autoignition. A later injection timing than that employed for hydrogen SI was found beneficial in the current study; HCCI of heptane/hydrogen mixtures was typically enabled with a SOI of 280° CA ATDC, in comparison to the SOI of 220° CA ATDC used for SI, *i.e.* a shift of 60° CA later. This could be related to the increased in-cylinder pressure and temperature at the later crank angle of injection offsetting any cooling, and/or to the later introduction of hydrogen yielding a certain degree of stratification beneficial for compression ignition.

The results in this section will be presented in terms of injection pulse-width (*i.e.* duration) of each fuel, rather than in terms of a global equivalence ratio or a global calorific content of the mixture. This seemed more suitable to the nature of the current study which aimed to investigate the impact of the relative composition of the heptane and hydrogen mixture on combustion and to identify practical means by which HCCI could be enabled on mixtures of these two fuels at various conditions. It is, however, quite important to identify quantitatively the relative AFRs involved. Therefore, Tables 4 and 5 show the air excess ratio that corresponded to the injection pulse-width adopted for each fuel in all the cases studied.

Table 4. Relationship between Injection Duration and AFR for Hydrogen DI, 70 bar.

Injection Pulse [ms]	6	8	10	12	14
Air Excess Ratio, λ	2.8	2.5	2.1	1.7	1.3

Table 5. Relationship between Injection Duration and AFR for Heptane PFI, 4 bar.

Injection Pulse [ms]	1.3	1.8	2.5	2.9	4.0
Air Excess Ratio, λ	3.5	3.1	2.6	2.3	1.4

Figure 13 shows a series of HCCI mean pressure traces with pure heptane and mixtures of heptane and hydrogen. All tests were carried out with 200 °C intake air temperature. For heptane HCCI with injection duration of 2.9 ms and λ=2.3, the corresponding pressure trace in Figure 13 demonstrates the lower misfire limit of HCCI with sole heptane fuelling at the conditions run. In contrast, heptane HCCI with an injection duration of 4.0 ms and corresponding λ=1.4 is also shown in Figure 13 to define an upper limit of sole heptane fuelling for the same operating conditions (this

limit was dictated by safety issues related to the optical components of the engine). The mean pressure trace recorded for a mixture of heptane and hydrogen prepared with a heptane injection of 2.9 ms and ahydrogen injection duration of 6 ms is also shown in Figure 13. Furthermore, the mean in-cylinder pressure trace of 6 ms hydrogen injection combined with 2.5 ms heptane injection has also been included in Figure 13. These traces were selected to demonstrate the effect of fixing the duration of heptane's injection and then adding hydrogen to it, as well as fixing the duration of hydrogen injection and then changing heptane's injection duration.

It can easily be observed in Figure 13 that although the 2.9 ms pure heptane injection is not producing much work (in comparison to the also shown motoring pressure trace), when 6 ms of hydrogen is added to it, this develops into a combustion event that has an in-cylinder pressure that is very similar to that recorded for the 4.0 ms sole heptane HCCI combustion, albeit slightly delayed and with a slower rate of autoignition. By keeping now fixed the injection duration of hydrogen at 6 ms and decreasing the injection duration of heptane down to 2.5 ms, it seems that there is a quite strong effect of the lack of these 0.4 ms of heptane; eventually this mixture led to a 10 bar decrease in peak pressure and much slower speed of autoignition in Figure 13. This effect is also manifested as a delay of about 10° CA in the start of the main combustion event, although the cool flame part remains quite similar to that of the 2.9 ms heptane, 6 ms hydrogen mixture. The fact that the cool flame part is similar for pure heptane HCCI with 4.0 ms injection duration and the mixture formed by 2.9 ms of heptane injection and 6 ms of hydrogen (although the cool flame of pure heptane with 2.9 ms injection duration is almost not even there on the corresponding pressure trace in Figure 13), might suggest that there is a strong effect of hydrogen's autoignition chemistry on the cool flame mechanism. In Figure 14, the rate of heat release shows more clearly the trends that evolved from the pressure data and the respective phasings of the cool flame and main combustion.

Figure 15 further illustrates the effects of hydrogen addition to heptane. Over the course of these experiments, the main focus was on gradually reducing the length of heptane's injection duration and increasing the duration of hydrogen injection in order to move closer to sole hydrogen HCCI operation. The results shown in Figure 15 illustrate that an increased injection duration of hydrogen does not necessarily lead to improved HCCI combustion when not supported by a proportionally adequate pilot injection of heptane. With a fixed heptane pilot injection of 1.8 ms (corresponding to λ=3.1), the addition of an extra 2 ms of hydrogen (from 10 ms to 12 ms, *i.e.* a change from λ=2.1 to λ=1.7) still promotes HCCI combustion. However, with a fixed heptane pilot injection of 1.3 ms, corresponding to λ=3.5, an extra 2 ms of hydrogen (from 12 ms to 14 ms, *i.e.* a change from λ=1.7 to λ=1.3) clearly suppresses HCCI combustion.

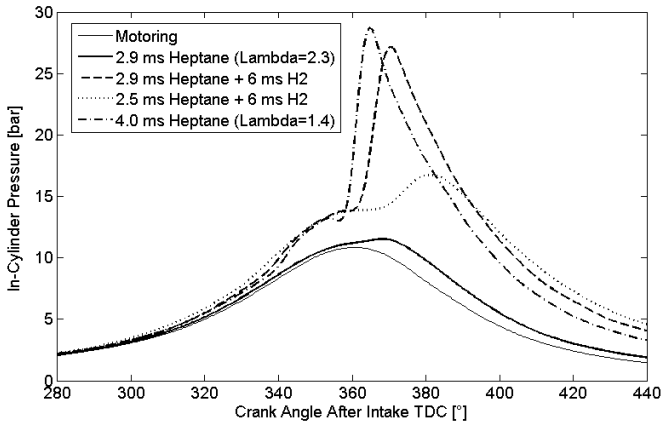

Figure 13. Effect of Hydrogen Injection on In-Cylinder Pressure for HCCI of Mixtures of Heptane and Hydrogen (200 °C, Heptane PFI with SOI 360° CA ATDC, Hydrogen DI with SOI 280° CA ATDC).

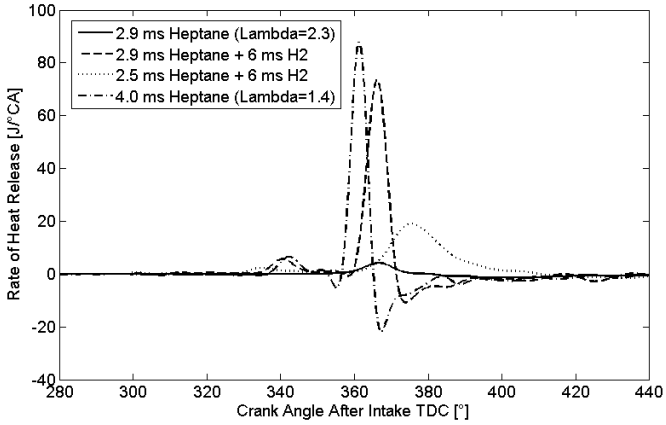

Figure 14. Effect of Hydrogen Injection on Rate of Heat Release for HCCI of Mixtures of Heptane and Hydrogen (200 °C, Heptane PFI with SOI 360° CA ATDC, Hydrogen DI with SOI 280° CA ATDC).

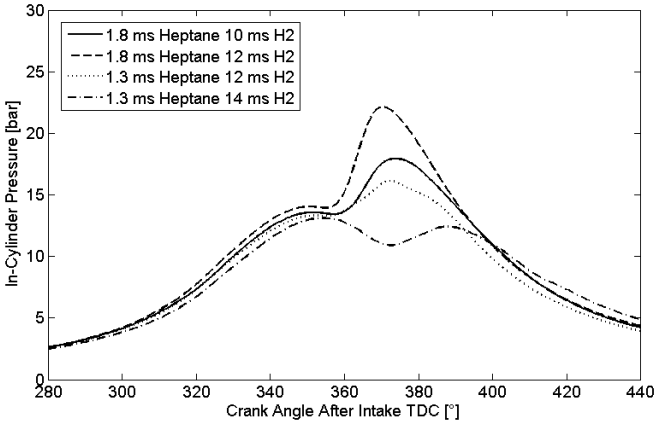

Figure 15. Effect of Hydrogen Injection on In-Cylinder Pressure for HCCI of Mixtures of Heptane and Hydrogen (200°, Heptane PFI with SOI 360° CA ATDC, Hydrogen DI with SOI 280° CA ATDC).

From the matrix of tests conducted, it emerged that the composition, as well as overall AFR of the mixture, have strong impact on the combustion development. As extensively documented by previous work, hydrogen or gas mixtures containing hydrogen, such as methanol reformed gas and hydrogen rich gas, have proved to be an excellent additive to control the knock, extend the lean limit, the tolerance to EGR and improve engine variability in SI engines [15, 35, 39]. When added to HCCI fuels with low octane number such as DME, hydrogen addition has been shown to act as a rather effective means by which it is possible to control the start of combustion by affecting the low temperature oxidation process [72–75]. Specifically, on a fixed amount of DME, addition of hydrogen seemed to slow down and in some cases suppress the first heat release stage (without changing its phasing though) by converting the more reactive OH radicals into HO_2 and H_2O_2 [75]. Because of the slower heat release during the low temperature oxidation period, the main combustion event was also delayed but it was not strongly affected in terms of peak pressure. The same trend was observed by fixing the overall equivalence ratio and changing the proportions of DME and hydrogen in the range 0% DME up to 50% DME and 50% hydrogen. However, at the lowest proportion of DME in the mixture, with 40% DME and 60% hydrogen, both the phasing and the magnitude of peak pressure were affected, with lower peak pressure values observed [73].

It is clear that these trends have to some extent been confirmed by the results of the present work and that hydrogen can act as a controlling agent on HCCI of heptane. However, there seems to be a difference in the fact that for constant heptane, hydrogen addition affected positively the peak pressure and advanced the phasing of the main combustion event (Figure 13 and 15). Additionally, for the combination of the lowest amount of heptane injected and largest amount of hydrogen, the effect was in fact negative, with hydrogen delaying the main combustion event to the point that the in-cylinder conditions no longer allowed for its development (Figure 15).

For completeness, one should take into account that the low compression ratio adopted in this study may have played an important role in the combustion development because when combined with the air pre-heating system, it was just sufficient enough to bring the mixtures to autoignition. In HCCI combustion of heptane, typically the second heat release stage (*i.e.* main combustion) is driven more by mixture composition rather than by temperature and it is believed that a high enough compression ratio is needed for the main combustion to develop. It must also be pointed out that at this stage of the experiments, with the adopted set-up, sole hydrogen fuelling did not lead to autoignition at any conditions of AFR or intake air temperature up to 200 °C. Therefore, the results presented so far led to an important conclusion related to HCCI combustion of heptane and hydrogen mixtures; the overall octane number of the mixture was not the only factor to favour autoignition. It can be speculated that the coexistence of the two fuels when the cool combustion of heptane occurs, promotes some mechanism of interaction between radicals of heptane's oxidation mechanism and hydrogen. The trigger of this process of autoignition resided somewhere between 340–360° CA ATDC.

Hydrogen Single Injection: The series of tests conducted with the aforementioned strategy helped to unveil a method to finally achieve pure hydrogen HCCI. It was understood that temperature, AFR, compression ratio and octane number of the mixture were not the only factors to be taken into account to reach the goal. Therefore, it was decided to increase the rate of internal EGR by changing the valve timing from Stage 1 to Stage 2, as presented earlier in Table 2 and Figure 4. This led to negative valve overlap. The hydrogen injection pressure was also raised from 70 to 100 bar to shorten the pulse-widths, thus advance the end of injection and allow time for better mixing and larger degree of homogeneity. Lastly the intake air heater was set up to achieve air preheat temperatures up to 400 °C. The synergy of these new operating conditions permitted to successfully enable pure hydrogen HCCI in the range of intake temperatures 200–400 °C. Assuming that the increased injection pressure played probably only a minor part, it could be speculated that the trapped residual gases were the key to promote the mechanism of this rather unusual combustion mode.

Figure 16 and Figure 17 show in-cylinder pressure traces and rates of heat release, respectively, at conditions of sole hydrogen HCCI for different air excess ratios in the range λ=1.6–2.0 and with a fixed intake temperature of 300 °C. At this temperature, λ=2.0 represented the lean limit as dictated by the minimum sufficient flame cheluminescence recorded in simultaneously acquired flame images. However, it was possible to sustain sole hydrogen HCCI combustion at λ=3.0 with a higher intake temperature of 400 °C. λ=1.6 was set as the rich limit for this study in order to avoid damage to the optical components of the engine, especially at the high temperatures involved. In Figures 16 and 17, both the autoignition phasing and rate of heat release don't seem to be strongly affected by the equivalence ratio in the range λ=1.8–2.0. However, for λ=1.6 the start of heat release occurs at around 330° CA ATDC and reaches its peak earlier than the other two mixtures, whilst being also wider. As a consequence peak pressure occurs later for λ=1.6 than that of the other two mixtures, namely at about 375° CA, which is about 10° CA later than that for λ=1.8 and λ=2.0.

A similar analysis of different equivalence ratios at a fixed intake air temperature can be found in the modelling study of Kominos *et al.* [89]. Specifically, the latter authors presented in-cylinder pressures with an AFR sweep at 2000 RPM, a compression ratio of 19 and an intake air temperature of 127 °C. Their results showed that a change from λ=5.0 to λ=2.5 led to a 12°

CA advance in the autoignition timing and to 25 bar increase in peak pressure. Bearing in mind the substantial difference in compression ratio between the current study and [89], it can be said that the behaviour presented in Figure 16 is qualitatively consistent.

The effect of intake air temperature on a fixed AFR is presented in Figure 18. As shown, the effect of temperature in the range 200–400 °C for λ=1.6 is not very strong. Similar degree of sensitivity was observed for leaner fuelling too. It is evident that a 200 °C raise in intake temperature is just enough to produce a sizeable shift in the phasing of autoignition and a 2.5 bar increase in peak in-cylinder pressure, without much difference in the angle of peak pressure. For comparison, a 20 °C increase in intake air temperature for sole heptane HCCI with λ=1.4, advanced the autoignition angle by 10° CA and increased the peak pressure by about 3 bar as shown earlier in Figure 11.

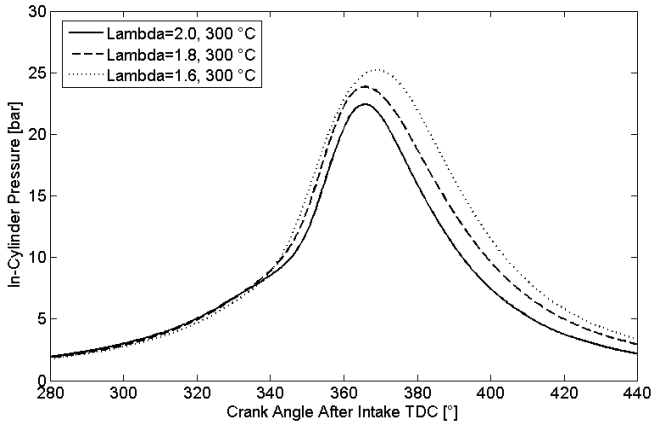

Figure 16. Effect of AFR on In-Cylinder Pressure for HCCI of Hydrogen (300 °C, Hydrogen DI with SOI 280° CA ATDC).

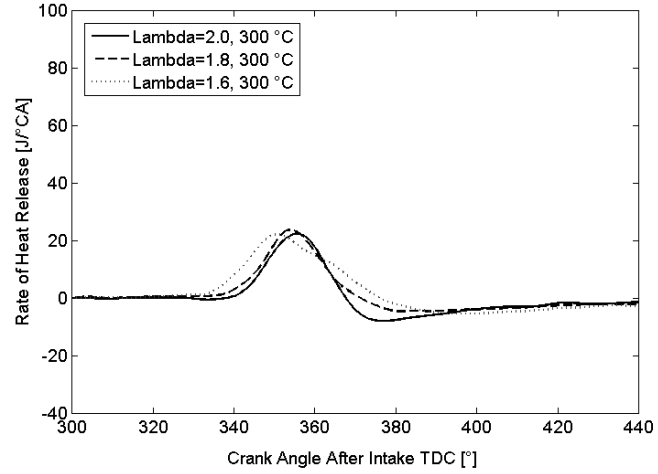

Figure 17. Effect of AFR on Heat Release Rate for HCCI of Hydrogen (300 °C, Hydrogen DI with SOI 280° CA ATDC).

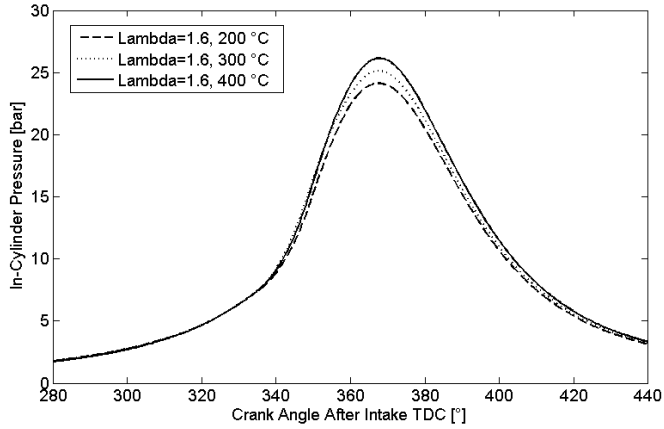

Figure 18. Effect of Intake Temperature on In-Cylinder Pressure for HCCI of Hydrogen (λ=1.6, Hydrogen DI with SOI 280° CA ATDC).

As already mentioned, the literature on sole hydrogen HCCI is scarce. Previous work consists mainly of two experimental studies [77, 78] and one modelling study [89]. These tests were carried out at high compression ratios ranging from 15:1 to 20:1, therefore some of the data are not directly comparable with the results of the current study. However, the trends related to intake air temperature and AFR observed here are not dissimilar from those documented by previous work, despite the absolute values of pressure and heat release being lower in the present study. Stenlåås *at al.* [77] presented a temperature sweep at λ=4.5, 1200 RPM and 17:1 compression ratio; for a difference of 10 °C, namely an increase from 107 °C to 117 °C, in-cylinder peak pressure rose from 45 to 60 bar and the ignition angle was advanced from 12° CA ATDC to 2° CA ATDC. By comparing these values with the observations linked to Figure 18, it is easy to understand that the compression ratio of the engine has a strong effect on the sensitivity of autoignition to intake temperature. In the modelling study of [89], for a compression ratio of 19 and 2000 RPM at λ=3.3, an increase in temperature at IVC of 15 °C (from 123 °C to 137 °C) was enough to advance the peak pressure by 10° CA and raise the peak value by 10 bar. Similar levels of temperature sensitivity have been reported in [78] for a compression ratio of 17 and 2000 RPM. The study of Stenlåås *at al.* [77] has also shown the effect of engine speed on required intake temperature to sustain hydrogen HCCI combustion. These authors showed that at lower engine speeds, higher intake temperature was needed. Specifically at λ=4.5, when engine speed was dropped from 1600 RPM to 800 RPM, an increase in intake air temperature of 20 °C was needed to sustain HCCI. This is the opposite to what has been observed in HCCI of hydrocarbons. However, it seems that it can partly explain the large temperatures needed at the 1000 RPM speed selected for the current study, on top of the low compression ratio, in comparison to [77, 78, 89]. More to the point, in [77], when the compression ratio was dropped from 20:1 to 15:1, an increase in intake temperature from 80 °C to

150 °C was required to enable HCCI. On this trend line, assuming linearity over a wider range, it appears that it is rather normal that temperatures of up to 400 °C were needed for successful HCCI considering the compression ratio of 7.5:1 used in the current study.

Finally, Figure 19 shows a direct comparison between hydrogen HCCI and SI. Considering the non-optimised spark advance for SI at the wide-open-throttle conditions shown, the pressure traces of SI and HCCI look broadly similar for λ=2.0. The lean limit of operation was also about the same for SI and HCCI (around λ=3.0). It remains to be seen whether these two modes of combustion lead to different exhaust emissions; this is currently under study and will be presented in a future publication. For completeness, it needs to be noted that the data in Figure 19 were acquired from the engine in pure thermodynamic mode, *i.e.* without optical access. This led to slightly higher peak pressures than in optical mode for same AFR due to differences in heat transfer.

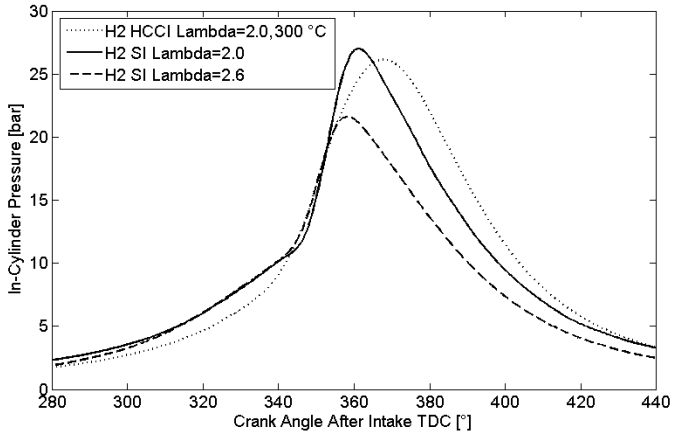

Figure 19. Comparison of In-Cylinder Pressure Traces for SI and HCCI of Hydrogen (DI with SOI 280° CA ATDC, Spark Advance 15° CA).

Hydrogen Multiple Injections: As it has already been discussed, sole hydrogen HCCI resulted from a combination of factors driven by injection timing, air preheating and the interaction of residuals with fresh charge. The chosen SOI of 280° CA ATDC was dictated by several constraints: it couldn't be advanced as it was bound by IVC timing and it would also cool excessively the charge, but it couldn't be retarded either because this wouldn't allow enough mixing time before ignition. In order to further investigate this aspect it was decided to attempt splitting the injection event into two smaller pulses, whilst keeping the total amount of fuel delivered per cycle the same. The strategy consisted of an early pulse with SOI=260° CA ATDC and a second pulse with SOI=310° CA ATDC. Figure 20 illustrates both the single and double injection pulses on the same graph of valve timings and motoring pressures for better understanding. The single injection for λ=1.8 lasts for 8 ms, *i.e.* 48° CA at 1000 RPM. For comparison, the double injection was split into two pulses; the first had a duration of 5.0 ms, *i.e.* 30° CA, whilst the second was 3.5 ms, *i.e.* 21° CA.

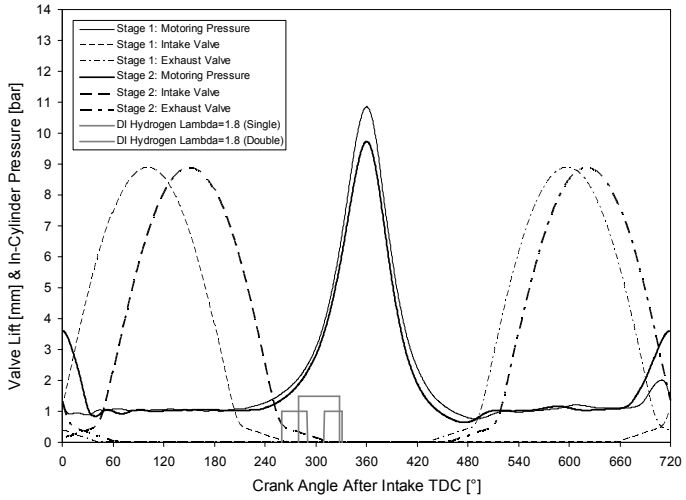

Figure 20. Hydrogen Direct Injection Timings and Durations in Comparison to Valve Timings.

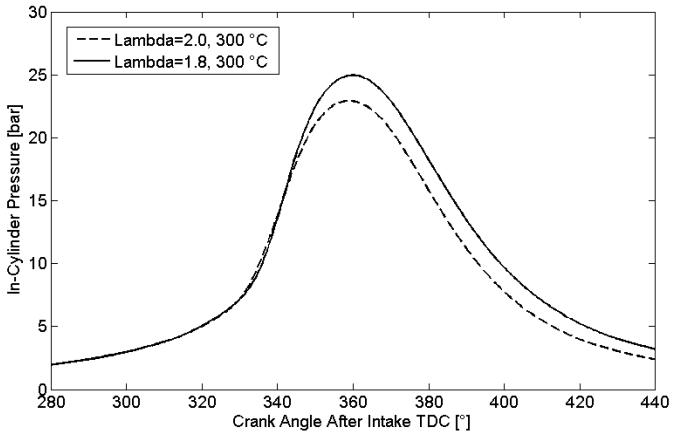

Figure 21. Effect of AFR on In-Cylinder Pressure for HCCI of Hydrogen (300 °C, Hydrogen Double DI with SOI 260° and 310° CA ATDC).

Figure 21 shows the effect of the double injection on in-cylinder pressure. It is noted that peak pressure reached similar or higher values when compared to single injection for the same AFR and intake air temperature (Figure 16). The main feature, however, is the different ignition angle; split injection led to advanced ignition when compared to the traditional single-injection strategy but the location of peak pressure was only marginally advanced from that of single injection. By studying Figures 20 and 21, it can be pointed out that autoignition begins when the second pulse of injection finishes. Flame imaging to be presented in the next section verified this. This observation of much earlier autoignition needs further study because it is considered quite peculiar. Although certain reasoning cannot be provided for such an unusual early ignition on the basis

of the current set of data, it can be speculated that the effect of splitting the injection event leads to a different mixing process between hydrogen and in-cylinder gas; whether this mechanism can be linked to phenomena analogous to Diesel engine autoignition processes with pilot injection is yet to be understood. However, it seems that by selecting different multiple injection strategies, with optimised injection pressure and mass flow, it could be possible to phase the start of autoignition to match different engine loads and speed requirements.

High-Speed Imaging

Heptane: Figure 22 shows typical flame images for different intake air temperatures and AFRs for heptane fuelling. It was observed that, irrespective of the magnitude of intake air temperature or AFR, the first autoignition site typically developed on the left hand-side of the combustion chamber on the image and close to the cylinder walls. Then combustion development proceeded in either growth of the first site or after generation of a second autoignition site very close to the first one leading ultimately to multiple autoignition site development. No specific pattern of autoignition was found to be more common than another, *i.e.* there were cycles with preferential single autoignition growth and others with multiple. Nevertheless, all of them originated on the same side of the combustion chamber as noted above. As far as trends are concerned with respect to AFR and temperature, it seems that the effect of AFR is stronger at higher temperatures. The reader is also referred to Figures 9 and 11 for respective pressure traces. For example, at λ=1.4 the start of autoignition is advanced for the higher temperature of 200 °C in comparison to 180 °C. There is consistently a 6–7° CA difference in enflamed areas of similar size, *e.g.* compare images at 2° CA BTDC for 200 °C with images at 5° CA ATDC for 180 °C. Similar behaviour has been observed in other optical engines of low compression ratio with heptane fuelling at analogous operating conditions [61–64], therefore, because this part of work was a stepping stone towards hydrogen HCCI, no more analysis will be carried out on the presented images within the bounds of the current publication.

Heptane/Hydrogen Mixtures: Figure 23 shows images of autoignition development for mixtures of hydrogen and heptane. The reader is referred to the pressure traces shown earlier in Figure 15 for the same operating conditions. The effects of hydrogen percentages into the mixture are evident in the corresponding images. With a fixed heptane injection of 1.8 ms (λ=3.1) the effect of increasing the injection duration of hydrogen from 10 ms to 12 ms (*i.e.* from λ=2.1 to 1.7, respectively) is critical in providing faster autoignition development manifested also by a brighter flame despite the higher individual values of λ involved. However, with a shorter pilot injection of heptane (1.3 ms, λ=3.5), when increasing the injection duration of hydrogen from 12 ms to 14 ms (*i.e.* from λ=1.7 to 1.3, respectively) the effect is a delay in the speed of autoignition development. It is also worth noting that in all HCCI images of mixtures of heptane and hydrogen, the patterns of autoignition changed in comparison to sole heptane HCCI. Autoignition did not start consistently from the left-hand-side of the combustion chamber, but showed a more global distribution, both at its start and subsequent development. Multiple autoignition sites were more common with heptane/hydrogen mixtures than in the case of sole heptane HCCI.

These observations could be linked to the degree of homogeneity of several parameters within the overall in-cylinder charge. For example, previous work on sole heptane fuelling [61–64] has highlighted the role played by the location of hot gases in the cylinder prior to autoignition. Autoignition is more likely to start at the location of maximum interaction between the fuel mixture and the hot EGR gases. When the autoignition front 'propagates' from one end of the cylinder to the other without other autoignition fronts appearing in the unburned region in the cylinder, this is an indication of a uniform gradient of temperature or AFR ratio, or even radical concentration, with a maximum (or minimum) value at the average autoignition location. When multiple points of ignition appear at diverse locations within the cylinder, it is believed that this could be due to the inhomogeneity of one of the above-named parameters. Perhaps the occurrence of more cases of multiple autoignition sites in the case of hydrogen and heptane mixtures in comparison to sole heptane HCCI is an indication of a mixture with a different degree of inhomogeneity that may have originated from the mixing process between the directly injected hydrogen and the already existing heptane distribution in the cylinder.

Hydrogen: Columns 1–3 in Figure 24 show images of pure hydrogen autoignition with different intake air temperatures at fixed AFR, namely λ=2.0. The reader is again referred to earlier graphs of in-cylinder pressure traces at similar conditions (Figures 16, 18, 19). It can be observed that the change in intake air temperature from 200 °C to 300 °C had a stronger influence on the angle at which the first sign of flame chemiluminescence appeared in the images when compared to the change observed from 300 °C to 400 °C. It certainly needs to be pointed out that the mechanism of hydrogen autoignition is very different to that observed for either pure heptane or mixtures of heptane and hydrogen. Autoignition almost always started on the right-hand-side of the combustion chamber and followed a clockwise swirling path motion during development till it filled up most of the cylinder bore. This might have been due to the strong effect of momentum exchange between the hydrogen DI jets (at the 100 bar injection pressure employed) and the in-cylinder charge. The reader needs to bear in mind that the end of single injection on this occasion was just prior to the start of autoignition (see Figure 20 for respective injection timing and duration). This might have also led to strong stratification of the in-cylinder charge, partly supported by the flame development images in Figure 24.

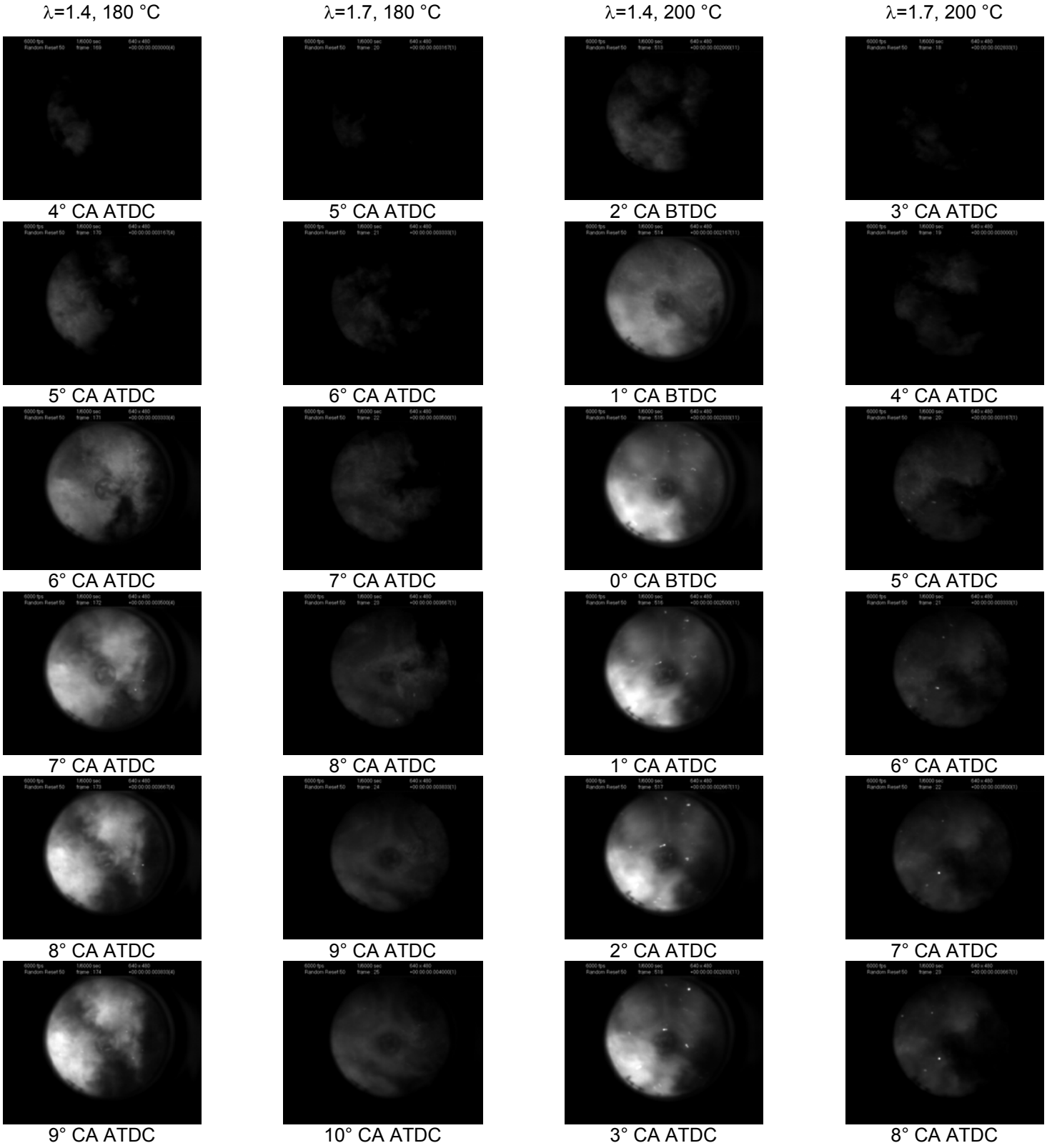

Figure 22. HCCI Flame Development of Heptane PFI (Intake Valves at the Top, Exhaust Valves at the Bottom).

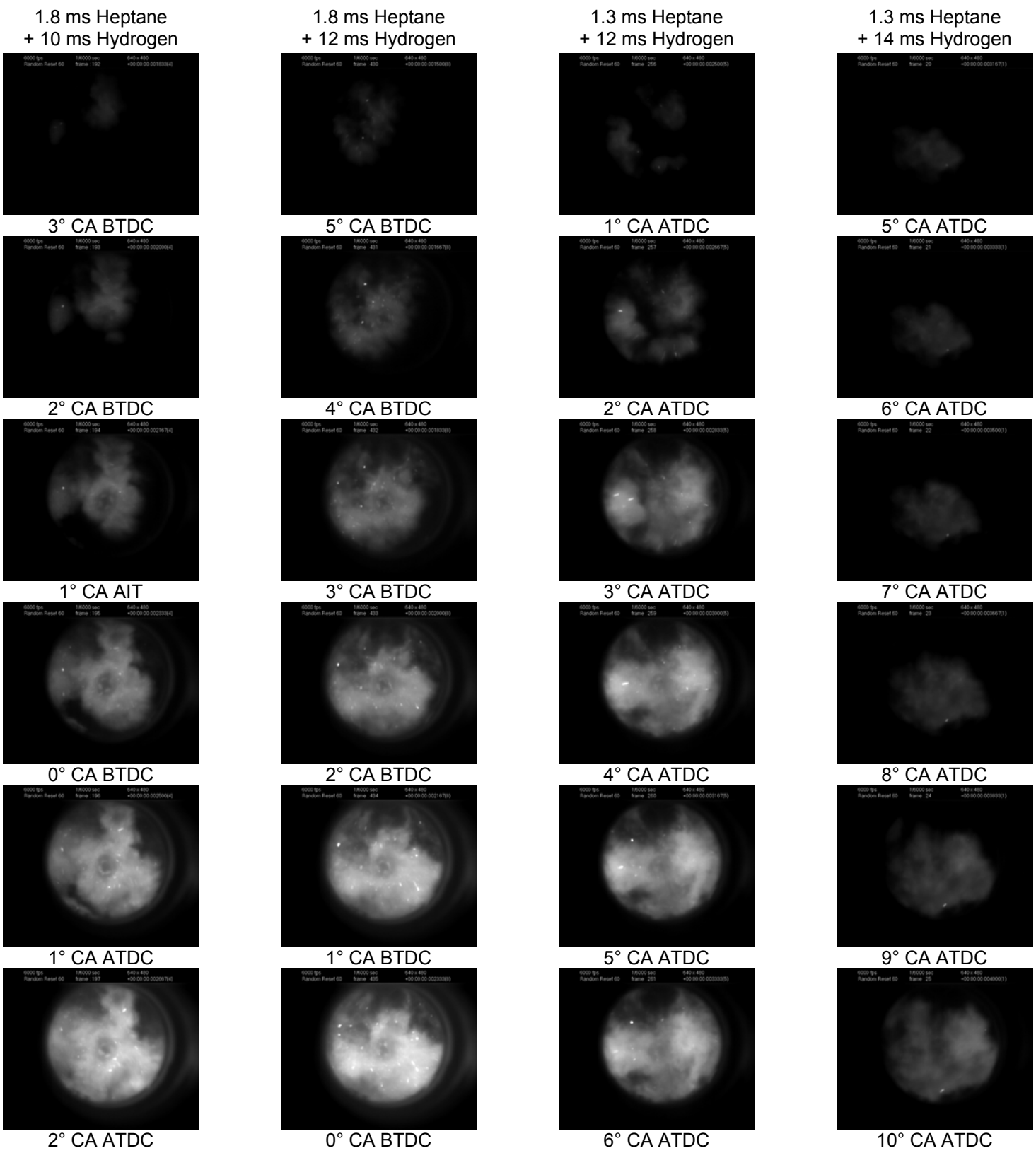

Figure 23. HCCI Flame Development of Heptane PFI and Hydrogen DI, Intake Temperature 200 °C (Intake Valves at the Top, Exhaust Valves at the Bottom).

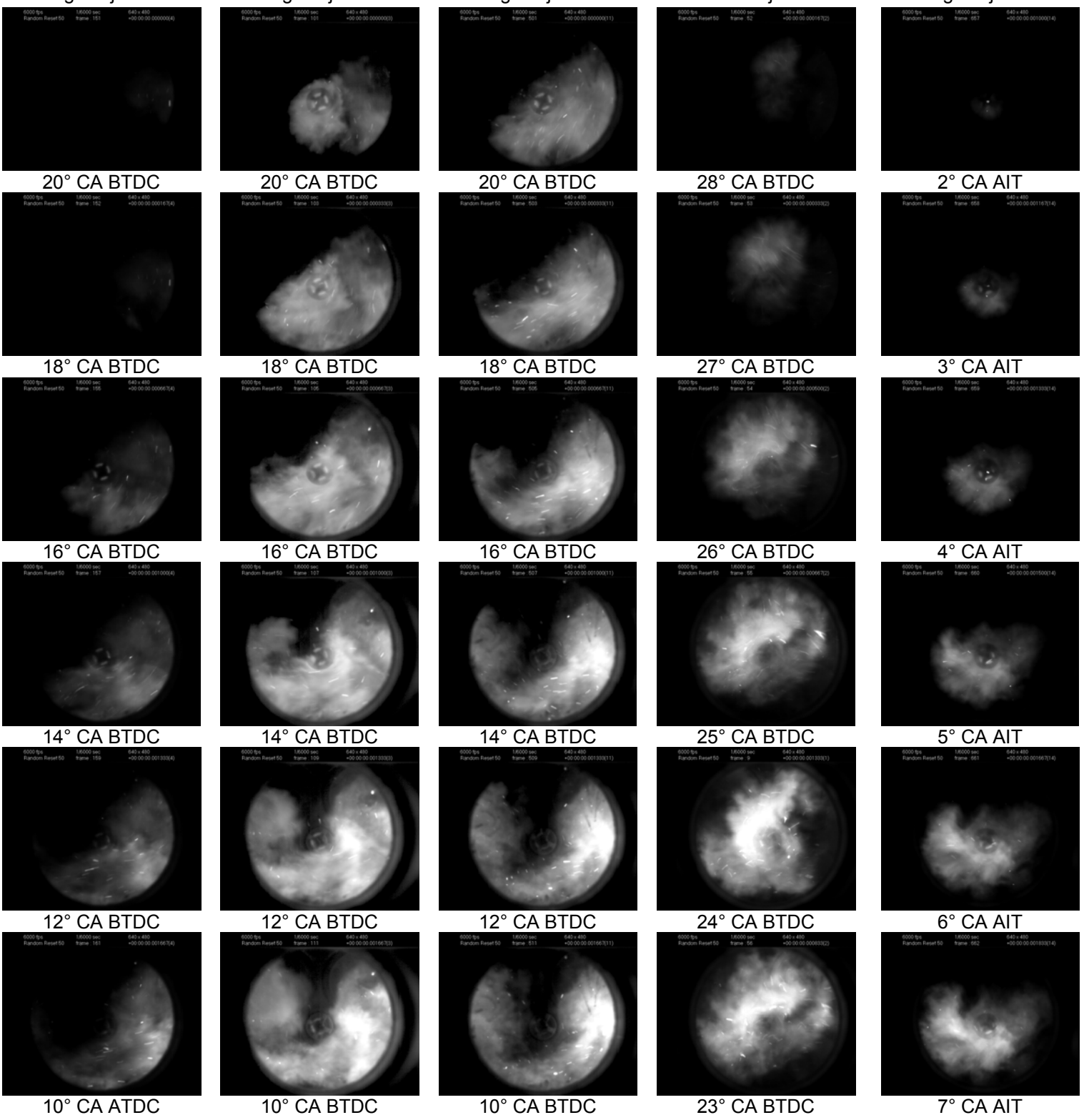

Figure 24. HCCI and SI Flame Development of Hydrogen DI, λ=2.0, Single Injection with SOI=280° CA ATDC, Double Injection with SOI=260° CA and 310° CA ATDC (Intake Valves at the Top, Exhaust Valves at the Bottom).

In contrast, Column 4 in Figure 24 presents a typical cycle of hydrogen autoignition with double injection at λ=2.0 and 300 °C (see Figure 20 for respective double injection timings and durations). The influence of this strategy on the autoignition pattern can be clearly seen when comparing Column 4 to Column 2 in the same Figure (both at 300 °C intake temperarture). When double injection was employed, no swirling pattern was observed in the autoignition images. In fact, autoignition started always centrally and developed towards the walls, filling up the bore gradually. This can be probably explained by the much lower effect of the direct injection process itself on the existing in-cylinder gas, *i.e.* weaker momentum exchange between the hydrogen jets and the in-cylinder gas. Additionally, it is believed that the double injection promoted faster and better mixing of the injected hydrogen with the in-cylinder charge. As already discussed when the respective pressure traces were introduced in Figure 21, autoignition started for the double injection strategy very early, typically at about 30° CA BTDC, *i.e.* about 10° CA earlier than the single injection strategy flames.

Finally, Column 5 shows a spark-ignited flame at the same condition (λ=2.0, unthrottled, SOI=280° CA ATDC) for direct comparison with the HCCI images in Columns 1–3. It can be observed that the SI flame also followed a swirling pattern in its development. This was much different to the spherical growth observed earlier in Figure 8 for part-load SI at richer AFRs and with an earlier SOI (220° CA ATDC), which fortifies the assumption about the effect of late DI on in-cylinder mixture motion and degree of stratification. More to the point, double injection hydrogen SI flame development (not shown here) exhibited a more central growth than that shown in Column 5 of Figure 24, which was also akin to the central pattern of combustion development shown in Column 4 for the double-injection hydrogen HCCI process.

CONCLUSIONS

This study focused on hydrogen combustion in an optical research engine running at 1000 RPM. Thermodynamic data and flame images were analysed for a broad range of operating conditions, including different fuels, SI and HCCI modes of engine operation with various mixture preparation methods, such as PFI and DI with single and double pulses per cycle. The main objective was to build up this study towards achievement of the ultimate goal of pure hydrogen HCCI. Therefore, a variety of fuels was employed, namely gasoline and hydrogen for SI, as well as heptane, or mixtures of heptane with hydrogen, and finally pure hydrogen for HCCI. The conclusions of this work may be summarized as follows:

- Spark ignition of hydrogen at part load (0.5 bar intake pressure) exhibited a fairly spherical flame growth, over the range of AFR tested (λ=1.2–2.0) for both PFI and DI mixture formation strategies. DI led to faster flame growth and higher peak pressure when compared to PFI. It also eliminated problems related to backfire and low calorific value of the in-cylinder charge due to air displacement, thus it was deemed preferable for the purposes of further study towards HCCI mode of engine operation.

- HCCI was initially enabled with PFI heptane fuelling with intake air temperatures up to 200 °C and hydrogen was gradually added to this by DI in order to understand the effect that this had on the combustion process. The overall octane number of the heptane/hydrogen mixture was not the only factor to favour autoignition. The coexistence of the two fuels when the cool combustion of heptane occurred, promoted some mechanism of interaction between heptane's oxidation radicals and hydrogen. The trigger of this mechanism of autoignition resided somewhere between 340–360° CA ATDC.

- For fixed amount of injected heptane, hydrogen addition affected positively the peak pressure and advanced the phasing of the main combustion event. In fact, even heptane HCCI with λ=2.3 that was close to the misfire limit, emerged as a prominent combustion event after addition of 6 ms of hydrogen to it. However, by gradually decreasing the amount of injected heptane and increasing the amount of injected hydrogen, the effect was not always positive. For the combination of the lowest amount of heptane injected (λ=3.5) and largest amount of hydrogen (14 ms), the effect was negative, with hydrogen strongly delaying the main combustion event to the point that the in-cylinder conditions not longer allowed for its development.

- The series of tests conducted with the aforementioned strategies helped to unveil a method to finally achieve pure hydrogen HCCI. The synergy between a new rate of internal EGR (induced by a modified valve timing that allowed for negative valve overlap) and a higher injection pressure (100 bar instead of 70 bar) that was used to shorten the injection event and advance the end of injection, permitted to successfully enable pure hydrogen HCCI in a range of intake temperatures 200–400 °C and up to λ=3.0.

- For HCCI of pure hydrogen, the effect of intake temperature in the range 200–400 °C was relatively small for λ=1.6–2.0. In fact, a 200 °C raise in intake temperature was just enough to slightly advance the autoignition phasing and also lead to a 2.5 bar increase in peak in-cylinder pressure, without causing much difference in the phasing of peak pressure. For comparison, a 20 °C increase in intake air temperature for sole heptane HCCI with λ=1.4 advanced the autoignition angle by 10° CA and increased the peak pressure by about 3 bar.

- The hydrogen autoignition phasing and rate of heat release were both not strongly affected by AFR in the range λ=1.8–2.0. However, for λ=1.6 the start of

heat release occurred earlier (30° CA BTDC) and also reached its peak earlier than the other two mixtures, whilst being also wider. As a consequence peak pressure occurred later for λ=1.6 by 10° CA.

- HCCI combustion imaging revealed certain features of the heptane and hydrogen autoignition processes. For heptane, the first autoignition site typically developed on the left hand-side of the combustion chamber on the image and close to the cylinder walls. No specific pattern of autoignition was found to be more common than another, *i.e.* there were cycles with preferential single autoignition growth and others with multiple.

- Addition of hydrogen to heptane HCCI showed that the patterns of autoignition changed in comparison to sole heptane HCCI. Autoignition did not start consistently from the left-hand-side of the combustion chamber, but showed a more global distribution, both at its start and subsequent development. Multiple autoignition sites were more common than in the case of sole heptane HCCI. These observations could be linked to the degree of inhomogeneity of several parameters within the in-cylinder charge that may have originated from the mechanism of mixing between the directly injected hydrogen and the already existing heptane distribution in the cylinder.

- The mechanism of sole hydrogen HCCI was very different to that observed for either pure heptane or mixtures of heptane and hydrogen. Autoignition almost always started on the right-hand-side of the combustion chamber and followed a clockwise swirling path motion during development. This might have been due to the strong effect of momentum exchange between the hydrogen DI jets and the in-cylinder charge, as the end of injection was just prior to the start of autoignition. This might have also led to strong stratification of the in-cylinder charge, partly contributing to the preferential combustion development observed.

- To examine speculations with regards to the swirling development of hydrogen autoignition, a double injection strategy was adopted. In this case, no swirling pattern was observed in the combustion images and autoignition started always centrally and developed towards the walls. This can be probably explained by the weaker momentum exchange between the hydrogen jets of the two shorter pulses and the in-cylinder gas, as well as by faster and better mixing of the hydrogen. Autoignition on this occasion also started earlier than the single-injection strategy case.

- Comparison between SI flames at wide-open-throttle condition and AFR to that of HCCI revealed that SI flames also followed a swirling pattern in their development. This was much different to the spherical growth observed for part-load SI at richer AFRs and with an earlier SOI (220° CA ATDC). This fortified the assumption about the effect of late DI on in-cylinder mixture motion and degree of stratification.

ACKNOWLEDGMENTS

The authors would like to thank the Engineering and Physical Sciences Research Council (EPSRC) in the UK for financial support (grant EP/C520211/1) and Yasunori Shimada from KEIHIN Europe for supplying the gas port fuel injectors. The authors would also like to thank all members of the UCL Internal Combustion Engines Group for their assistance and many useful discussions.

REFERENCES

1. Cecil, W., “On the Application of Hydrogen Gas to Produce a Moving Power in Machinery; with a Description of an Engine which is Moved by the Pressure of the Atmosphere, upon a Vacuum Caused by Explosions of Hydrogen and Atmospheric Air”, Transactions of the Cambridge Philosophical Society, Vol. 1, pp. 217–240, 1822.
2. Das, L. M., “Hydrogen Engines: A View of the Past and a Look into the Future”, International Journal of Hydrogen Energy, Vol. 15, pp. 425–443, 1990.
3. Lee, S., Yoon, K., Han, B., Lee, H., Kwon, B., “Development of Hyundai Hydrogen-Fuelled Vehicle”, SAE Paper 952764, 1995.
4. Nakajima, Y., Yamane, K., Shudo, T., Hiruma, M. and Takagi, Y., “Research and Development of a Hydrogen-Fuelled Engine for Hybrid Electric Vehicles”, SAE Paper 2000-01-0993, 2000.
5. Taxon, M.N., Brueckner, S.R. and Bohac, S.V., “Effect of Fuel Humidity on the Performance of a Single-Cylinder Research Engine Operating on Hydrogen”, SAE Paper 2002-01-2685, 2002.
6. Stockhausen, W.F., Natkin, R.J., Kabat, D.M., Reams, L., Tang, X., Hashemi, S., Szwabowski, S.J. and Zanardelli, V.P., “Ford P2000 Hydrogen Engine Design and Vehicle Development Program”, SAE Paper 2002-01-0240, 2002.
7. Szwabowski, S.J., Shashemi, S., Stockhausen, W.F., Natkin, R., Realms, L., Kabat, D. and Potts, C., “Ford Hydrogen Engine Powered P2000 Vehicle”, SAE Paper 2002-01-0243, 2002.
8. Shinagawa, T., Okumura, T., Furuno, S. and Kim, K.-O., “Effects Hydrogen Addition to SI Engine on Knock Behaviour”, SAE Paper 2004-01-1851, 2004.
9. Berckmüller, M., Rottengruber, H., Eder, A., Brehm, Elsässer, G., Müller-Alander, G. and Schwarz, C., “Potentials of a Charged SI-Hydrogen Engine”, SAE Paper 2003-01-3210, 2003.
10. Eichlseder, H., Wallner, T., Freymann, R. and Ringler, J., “The Potential of Hydrogen Internal Combustion Engines in a Future Mobility Scenario”, SAE Paper 2003-01-2267, 2003.
11. Rottengruber, H., Berckmüller, M., Elsässer, G., Brehm, N. and Schwarz, C., “Direct-Injection

Hydrogen SI-Engine – Operation Strategy and Power Density Potentials", SAE Paper 2004-01-2927, 2004.
12. Wimmer, A., Wallner, T., Ringler, J. and Gerbi, F., "H_2-Direct Injection – A Highly Promising Combustion Concept", SAE Paper 2005-01-0108, 2005.
13. Bleechmore, C. and Brewster, S., "Dilution Strategies for load and NO_X Management in a Hydrogen Fuelled Direct Injection Engine", SAE Paper 2007-01-4097, 2007.
14. Karim, G.A., "Hydrogen as a Spark Ignition Engine Fuel", International Journal of Hydrogen Energy, Vol. 28, pp. 569–577, 2003.
15. Conte, E. and Boulouchos, K., "Influence of Hydrogen-Rich-Gas Addition on Combustion, Pollutant Formation and Efficiency of an IC-SI Engine", SAE Paper 2004-01-0972, 2004.
16. Cracknell, R.F., Alcock, J.L., Rowson, J.J., Shirvill, L.C. and Üngüt, A., "Safety Considerations in Retailing Hydrogen", SAE Paper 2002-01-1928, 2002.
17. Bradley, D., Lawes, M., Liu, K., Verhelst, S. and Woolley, R., "Laminar Burning Velocities of Lean Hydrogen-Air Mixtures at Pressures up to 1.0 MPa", Combustion and Flame, Vol. 149, pp. 162–172, 2007.
18. Mandilas, C., Ormsby, M.P., Sheppard, C.G.W. and Woolley, R., "Effects of Hydrogen Addition on Laminar and Turbulent Premixed Methane and Iso-Octane–Air Flames", Proceedings of the Combustion Institute, Vol. 31, pp. 1443–1450, 2007.
19. Lee, S.J., Yi, H.S. and Kim, E.S., "Combustion Characteristics of Intake Port Injection Type Hydrogen Fuelled Engine", International Journal of Hydrogen Energy, Vol. 20, pp. 317–322, 1995.
20. Norbeck, J.M., Heffel, J., Durbin, T., Montano, M., Tabbara, B. and Bowden, J., "Hydrogen Fuel for Surface Transportation", SAE, Warrendale, PA, USA, 1996.
21. White, C.M., Steeper, R.R, and Lutz, A.E., "The Hydrogen-Fueled Internal Combustion Engine: A Technical Review", International Journal of Hydrogen Energy, Vol. 31, pp. 1292–1305, 2006.
22. Verhelst, S., Sierens, R. and Verstraeten, S., "A Critical Review of Experimental Research on Hydrogen Fueled SI Engines", SAE Paper 2006-01-0430, 2006.
23. Verhelst, S., Verstraeten, S. and Sierens, R., "A Comprehensive Overview of Hydrogen Engine Design Features" Proceedings of IMechE, Part D, Journal of Automobile Engineering, Vol. 221, pp. 911–920, 2007.
24. Ingersoll, J.G., "Natural Gas Vehicles", Fairmont Press, 1996.
25. Li, H. and Karim, G.A., "Knock in Spark Ignition Hydrogen Engines", International Journal of Hydrogen Energy, Vol. 29, pp. 859–865, 2004.
26. Dwyer, H.A., McCaffey, Z. and Miller, M., "Analysis and Prediction of In-Cylinder NO_X Emissions for Learn-Burn CNG/Hydrogen Transit Bus Engines", SAE Paper 2004-01-1994, 2004.
27. Apostolescu, N. and Chiriac, R., "A Study of Combustion Hydrogen-Enriched Gasoline in a SI Engine", SAE Paper 960603, 1996.
28. Suzuki, T. and Sakurai, Y., "Effect of Hydrogen Rich Gas and Gasoline Mixed Combustion on Spark Ignition Engine", SAE Paper 2006-01-3379, 2006.
29. Akansu, O.S., Dulger, Z., Kahraman, N. and Vezirogklu, T.N., "Internal Combustion Engines Fuelled by Natural Gas-Hydrogen Mixtures", International Journal of Hydrogen Energy, Vol. 29, pp. 1527–1539, 2004.
30. Hoekstra, R.L., van Blarigan, P. and Mulligan, N., "NO_X Emissions and Efficiency Hydrogen, Natural gas and Hydrogen/Natural Gas Blended Fuels", SAE Paper 961103, 1996.
31. Tunestål, P., Christensen, M., Einewall, P., Andersson, T., Johansson, B. and Jonsson, O., "Hydrogen Addition for Improved Lean-Burn Capability of Slow and Fast Burning Natural Gas Combustion Chambers", SAE Paper 2002-01-2686, 2002.
32. Li, H. and Karim, G.A., "An Experimental Investigation of SI Engine Operation on Gaseous Fuels Lean Mixtures", SAE Paper 2005-01-3765, 2005.
33. Heffel, J.W., "NO_X Emission and Performance Data for a Hydrogen Fueled Internal Combustion Engine at 1500 RPM using Exhaust Gas Recirculation", International Journal of Hydrogen Energy, Vol. 28, pp. 901–908, 2003.
34. Heffel, J.W., "NO_X Emission and Performance Data for a Hydrogen Fueled Internal Combustion Engine at 3000 RPM using Exhaust Gas Recirculation", International Journal of Hydrogen Energy, Vol. 28, pp. 1285–1292, 2003.
35. Topinka, J.A., Gerty, M.D., Heywood, J.B. and Keck, J.C., "Knock Behavior of a Lean-Burn, Hydrogen and CO Enhanced, SI Gasoline Engine Concept", SAE Paper 2004-01-0975, 2004.
36. Ivanič, Z., Ayala, F., Goldwitz, J. and Heywood, J.B., "Effects of Hydrogen Enhancement on Efficiency and NO_X Emissions of Lean and EGR-Diluted Mixtures in a SI Engine", SAE Paper 2005-01-0253, 2005.
37. Verhelst, S., De Landtsheere, J., De Smet, F., Billiouw, C., Trenson, A. and Sierens, R., "Effects of Supercharging, EGR and Variable Valve Timing on Power and Emissions of Hydrogen Internal Combustion Engines", SAE Paper 2008-01-1033, 2008.
38. Nande, A.M., Szwaja, S. and Naber, J.D., "Impact of EGR on Combustion Processes in a Hydrogen Fuelled SI Engine", SAE Paper 2008-01-1039, 2008.
39. Allgeier, T., Klenk, M., Landenfeld, T., Conte, E., Boulouchos, K. and Czerwinski, J., "Advanced Emission and Fuel Economy Concept Using Combined Injection of Gasoline and Hydrogen in SI-Engines", Sae Paper 2004-01-1270, 2004.

40. Alger, T., Gingrich, J. and Mangold, B., “The Effect of Hydrogen Enrichment on EGR Tolerance in Spark Ignited Engines”, SAE Paper 2007-01-0475, 2007.
41. Das, L.M., Gulati, R. and Gupta, P.K., “A Comparative Evaluation of the Performance Characteristics of a SI Engine Using Hydrogen and Compressed Natural Gas as Alternative Fuels”, International Journal of Hydrogen Energy, Vol. 25, pp. 783–793, 2000.
42. Das, L.M., Gulati, R. and Gupta, P.K., “Performance Evaluation of a Hydrogen-Fuelled SI Engine Using Electronically Controlled Solenoid-Actuated Injection System”, International Journal of Hydrogen Energy, Vol. 25, pp. 569–579, 2000.
43. Heffel, J.F., Johnson, D.C. and Shelby, C., “Hydrogen Powered Shelby Cobra: Vehicle Conversion”, SAE Paper 2001-01-2530, 2001.
44. Heffel, J.W., McClanahan, M.N., Norbeck, J.M. and Lynch, F.E., “Turbocharged Hydrogen Fuelled Vehicle Using Constant Volume Injection”, SAE Paper 981922, 1998.
45. Kölsch, R.K. and Clark, S.J., 1979, “A Comparison of Hydrogen and Propane Fuelling of an IC Engine”, SAE Paper 790677, 1979.
46. Verhelst, S. and Sierens, R., “Combustion Studies for PFI Hydrogen IC Engines”, SAE Paper 2007-01-3610, 2007.
47. Wallner, T. and Lohse-Busch, H., “Performance, Efficiency and Emissions Evaluation of a Supercharged, Hydrogen-Powered, 4-Cylinder Engine”, SAE Paper 2007-01-0016, 2007.
48. Guo, L.S., Lu, H.B. and Li, J.D., “A Hydrogen Injection System with Solenoid Valves for a Four-Cylinder Hydrogen-Fuelled Engine”, International Journal of Hydrogen Energy, Vol. 24, pp. 377–382, 1999.
49. Meier, F., Köhler, J., Stolz, W., Bloss, W.H. and Al-Garni, M., “Cycle-Resolved Hydrogen Flame Speed Measurements with High-Speed Schlieren Technique in a Hydrogen Direct Injection SI Engine”, SAE Paper 942036, 1994.
50. Yi, H.S., Lee, S.J. and Kim, E.S., “Performance Evaluation and Emission Characteristics of In-Cylinder Injection Type Hydrogen Fuelled Engine”, International Journal of Hydrogen Energy, Vol. 21, pp. 617–624, 1996.
51. Heywood, J.B. and Vilchis, F.R., “Comparison of Flame Development in SI Engine Fuelled with Propane and Hydrogen”, Combustion Science and Technology, Vol. 38, pp. 313–324, 1984.
52. Meier, F., Wiltafsky, G., Köhler, J. and Stolz, W., “Quantitative Time Resolved 2D Fuel-Air Ratio Measurements in a Hydrogen Direct Injection SI Engine Using Spontaneous Raman Scattering”, SAE Paper 961101, 1996.
53. Koyanagi, K., Hiruma, M., Yamane, K. and Furuhana, S., “Effect of Hydrogen Jet on Mixture Formation in a High-Pressure Injection Hydrogen Fuelled Engine with Spark Ignition”, SAE Paper 931811, 1993.
54. Blotevogel, T., Egermann, J., Goldlücke, J., Leipertz, A., Hartmann, M. and Schenk, M. and Berckmüller, M., “Developing Planar Laser-Induced Fluorescence for the Investigation of the Mixture Formation Process in Hydrogen Engines”, SAE Paper, 2004-01-1408.
55. Kirchweger, W. and Haslacher, R., “Applications of the LIF Method for the Diagnostics of the Combustion Process of Gas-IC-Engines”, Experiments in Fluids, Vol. 43, pp. 329–340, 2007.
56. White, C.M., “A Qualitative Evaluation of Mixture Formation in a Direct-Injection Hydrogen-Fuelled Engine”, SAE Paper 2007-01-1467, 2007.
57. Wallner, T., Ciatti, S. and Bihari, B., “Investigation of Injection Parameters in a Hydrogen DI Engine Using an Endoscopic Access to the Combustion Chamber”, SAE Paper 2007-01-1464, 2007.
58. Wallner, T., Nande, A.M. and Naber, J., “Evaluation of Injector Location and Nozzle Design in a Direct-Injection Hydrogen Research Engine”, SAE Paper 2008-01-1785, 2008.
59. Thring, R.H., “Homogeneous-Charge Compression-Ignition (HCCI) Engines”, SAE 892068, 1989.
60. Kaiser, E.W., Yang, J., Culp, T., Xu, N. and Maricq, M.M., 2002, “Homogeneous Charge Compression Ignition Engine-Out Emissions – Does Flame Propagation Occur in HCCI?” International Journal of Engine Research, Vol. 3, pp. 185–195, 2002.
61. Aleiferis, P.G., Charalambides, A.G., Hardalupas, Y. Taylor, A.M.K.P. and Urata, Y., “Modelling and Experiments of HCCI Engine Combustion with Charge Stratification and Internal EGR”, SAE Paper 2005-01-3725, 2005.
62. Aleiferis, P.G., Charalambides, A.G., Hardalupas, Y. Taylor, A.M.K.P. and Urata, Y., “Autoignition Initiation and Development of n-Heptane HCCI Combustion Assisted by Inlet Air Heating, Internal EGR or Spark Discharge: An Optical Investigation”, SAE Paper 2006-01-3273, 2006.
63. Aleiferis, P.G., Charalambides, A.G., Hardalupas, Y., Taylor, A.M.K.P. and Urata, Y., “Axial Fuel Stratification of a Homogeneous Charge Compression Ignition (HCCI) Engine”, International Journal of Vehicle Design, Vol. 44, pp. 41–61, 2007.
64. Aleiferis, P.G., Charalambides, A.G., Hardalupas, Y. Taylor, A.M.K.P. and Urata, Y., “The Effect of Axial Charge Stratification and Exhaust Gases on Combustion Development in a Homogeneous Charge Compression Ignition Engine”, Proceedings of IMechE, Part D, Journal of Automobile Engineering, pp. 2171–2183, 2008.
65. Tsurushima, T., Harada, A., Iwashiro, Y., Enomoto, Y., Asaumi, Y. and Aoyagi, Y., “Thermodynamic Characteristics of Premixed Compression Ignition Combustions”, SAE Paper 2001-01-1891, 2001.
66. Christensen, M. and Johansson, B., “The Effect of In-Cylinder Flow and Turbulence on HCCI Operation”, SAE Paper 2002-01-2864, 2002.
67. Christensen, M., Hultqvist, A. and Johansson, B., “Demonstrating the Multi-Fuel Capability of a

Homogeneous Charge Compression Ignition Engine with Variable Compression Ratio", SAE 1999-01-3679, 1999.
68. Amann, M., Ryan III, T.W., Kono, N., "HCCI Fuels Evaluations – Gasoline and Diesel Boiling Ranges", SAE Paper 2005-01-3727, 2005.
69. Naber, J.D. and Siebers, D.L., "Hydrogen Combustion under Diesel Engine Conditions", International Journal of Hydrogen Energy, Vol. 23, p. 363–371, 1998.
70. Noda, T. and Foster, D.E., "A Numerical Study to Control Combustion Duration Hydrogen-Fuelled HCCI by Using Multi-Zone Chemical Kinetics Simulation", SAE Paper 2001-01-0250, 2001.
71. Lu, J., Gupta, A.K., Pouring, A.A. and Keating, E.L., "A Preliminary Study of Chemically Enhanced Autoignition in an Internal Combustion Engine", SAE Paper 940758, 1994.
72. Shudo, T. and Ono, Y., "HCCI Combustion of Hydrogen, Carbon Monoxide and Dimethyl Ether", SAE Paper 2002-01-0112, 2002.
73. Shudo, T., Ono, Y. and Takahashi, T., "Influence of Hydrogen and Carbon Monoxide on HCCI Combustion of Dimethyl Ether", SAE Paper 2002-01-2828, 2002.
74. Shudo, T. and Takahashi, T., "Influence of Reformed Gas Composition on HCCI Combustion of Onboard Methanol-Reformed Gases", SAE Paper 2004-01-1908, 2004.
75. Shudo, T. and Yamada, H., "Hydrogen as an Ignition-Controlling Agent for HCCI Combustion Engine by Suppressing the Low-Temperature Oxidation", International Journal of Hydrogen Energy, Vol. 32, pp. 3066–3072, 2007.
76. Yap, D., Megaritis, A., Peucheret, S., Wyszynski, M.L. and Xu, M., "Effect of Hydrogen Addition on Natural Gas HCCI Combustion", SAE Paper 2004-01-1972, 2004.
77. Stenlåås, O., Christensen, M., Egnell, R., Johansson, B. and Mauss, F., "Hydrogen as Homogeneous Charge Compression Ignition Engine Fuel", Paper 2004-01-1976, 2004.
78. Gomes Antunes, J.M., Mikalsen, R. and Roskilly, A.P., "An Investigation of Hydrogen-Fuelled HCCI Engine Performance and Operation", International Journal of Hydrogen Energy, Vol. 33, pp. 5823–5828, 2008.
79. Richter, M., Engström, J., Franke, A., Aldén, M., Hultqvist, A. and Johansson, B., 2000, "The Influence of Charge Inhomogeneity on the HCCI Combustion Process", SAE Paper 2000-01-2868.
80. Zhao, H., Peng, Z., Williams, J. and Ladommatos, N., "Understanding the Effects of Recycled Burnt Gases on the Controlled Autoignition (CAI) Combustion in Four-Stroke Gasoline Engines", SAE Paper 2001-01-3607, 2001.
81. Hultqvist, A., Christensen, M., Johansson, B., Richter, M., Nygren, J., Hult, J., Aldén, "The HCCI Combustion Process in a Single Cycle – High-Speed Fuel Tracer LIF and Chemiluminescence Imaging", SAE Paper 2002-01-0424, 2002.
82. Hultqvist, A., Christensen, M., Johansson, B., Franke, A., Richter, M., Aldén, M., "A Study of the Homogeneous Charge Compression Ignition Combustion Process by Chemiluminescence Imaging", SAE 1999-01-3680, 1999.
83. Steeper, R.R. and De Zilwa, S., "Improving the NO_X-CO_2 Trade-Off of an HCCI Engine Using a Multi-Hole Injector", 2007-01-0180. 2007.
84. Graf, N., Gronki, J., Schulz, C., Baritaud, T., Cherel, J., Duret, P.Lavy, J., "In-Cylinder Combustion Visualization in an Auto-Igniting Gasoline Engine using Fuel Tracer- and Formaldehyde-LIF Imaging", SAE Paper 2001-01-1924, 2001.
85. Collin, R., Nygren, J., Richter, M., Aldén M., Hildingsson, L. and Johansson, B., "Simultaneous OH and Formaldehyde LIF Measurements in an HCCI Engine", SAE Paper 2003-01-3218, 2003.
86. Peng, Z., Zhao, H. and Ladommatos, N., "Visualization of the Homogeneous Charge Compression Ignition/Controlled Autoignition Combustion Process Using Two-Dimensional Planar Laser-Induced Fluorescence Imaging of Formaldehyde", Proceedings of IMechE, Part D, Journal of Automobile Engineering, Vol. 217, pp. 1125–1134, 2003.
87. Mulenga, M.C., Ting, D.S.-K., Reader, G.T. and Zheng, M., "The Potential for Reducing CO and NO_X Emissions from an HCCI Engine Using H_2O_2 Addition", SAE Paper 2003-01-3204, 2003.
88. Wong, Y.K. and Karim, G.A., "An Analytical Examination of the Effects of Hydrogen Addition on Cyclic Variations in Homogeneously Charged Compression Ignition Engines", International Journal of Hydrogen Energy, Vol. 25, pp. 1217–1224, 2000.
89. Komninos, N.P., Hountalas, D.T. and Rakopoulos, C.D., "A Parametric Investigation of Hydrogen HCCI Combustion Using a Multi-Zone Model Approach", Energy Conversion and Management, Vol. 48, pp. 2934–2941, 2007.
90. Bisetti, F., Chen, J.-Y., Chen, J.H. and Hawkes, E.R., "Characterization of Differential Diffusion Effects during the Constant Volume Ignition of a Temperature Stratified Lean Premixed Hydrogen/Air Mixture Subject to Decaying Turbulence", Fall Meeting of the Western States Section of the Combustion Institute, Sandia National Laboratories, Livermore, CA, USA, October 16–17, 2007.
91. Markides, C.N. and Mastorakos, E., "An Experimental Study of Hydrogen Autoignition in a Turbulent Co-Flow of Heated Air", Proceedings of the Combustion Institute, Vol. 30, pp. 883–891, 2005.
92. Todd, A.R., "Optical Studies in a Firing Stratified-Charge GDI Engine", PhD Thesis, University of London, 2007.
93. Ohira, T., Nakagawa, K., Yamane, K., Kawanabe, H. and Shioji, M., "Feasibility Study of Emission Control of Hydrogen Fueled SI Engine", Proceedings of

IMechE International Conference on Internal Combustion Engines: Performance, Fuel Economy and Emissions, pp. 199–209, December 11–12, London, 2007.
94. Aleiferis, P.G., Malcolm, J.S., Cairns, A., Todd, A.R. and Hoffmann, H., “An Optical Study of Spray Development and Combustion of Ethanol, Iso-Octane and Gasoline Blends in a DISI Engine”, SAE Paper 2008-01-0073, 2008.
95. Serras-Pereira, J., Aleiferis, P.G., Richardson, D. and Wallace, S., “Characteristics of Ethanol, Butanol, Iso-Octane and Gasoline Sprays and Combustion from a Multi-Hole Injector in a DISI Engine”, SAE Paper 2008-01-1591, 2008.
96. Owston, R., Magi, V. and Abraham, J., “Fuel-Air Mixing Characteristics of DI Hydrogen Jets”, SAE Paper 2008-01-1041, 2008.
97. Utgikar, V.P. and Thiesen, T., “Safety of Compressed Hydrogen Fuel Tanks: Leakage from Stationary Vehicles”, Technology in Society, Vol. 27, pp. 315–320, 2005.

ABBREVIATIONS

AFR	Air to Fuel Ratio
AIT	After Ignition Timing
ATDC	After Top Dead Centre
BTDC	Before Top Dead Centre
CA	Crank Angle
CAI	Controlled Autoignition
CI	Compression Ignition
DI	Direct Injection
DNS	Direct Numerical Simulation
EGR	Exhaust Gas Recirculation
EVC	Exhaust Valve Closure
EVO	Exhaust Valve Open
HCCI	Homogeneous Charge Compression Ignition
IVC	Intake Valve Closure
IVO	Intake Valve Open
MBT	Minimum spark advance for Best Torque
MFB	Mass Fraction Burnt
MON	Motor Octane Number
PFI	Port Fuel Injection
RON	Research Octane Number
RPM	Revolutions Per Minute
SI	Spark Ignition
SOI	Start Of Injection
TDC	Top Dead Centre

CONTACT

Author for correspondence:

Dr. Pavlos Aleiferis
Department of Mechanical Engineering
University College London
Torrington Place
London WC1E 7JE
United Kingdom
E-mail: p_aleiferis@meng.ucl.ac.uk